Optimal Model Complexity in Geological Carbon Sequestration: A Design of Experiment (DoE) & Response Surface (RS) Uncertainty Analysis

DE-FE-0009238

Ye Zhang[1], Mingkan Zhang[1], Peter Lichtner[2]

1. Dept. of Geology & Geophysics, University of Wyoming, Laramie, Wyoming
2. OFM Research, Inc., Santa Fe, New Mexico

U.S. Department of Energy
National Energy Technology Laboratory
Strategic Center for Coal's
FY16 Carbon Storage Annual Review Meeting
August 16-18, 2016, Pittsburg, PA

Project Objectives

Overall Goals:

1. Support industry's ability to predict CO_2 storage capacity in geologic formations to within ±30% accuracy;
2. Develop and validate technologies to ensure 99% storage permanence.

Specific Objectives:

For GCS in environments with permeability (*k*) heterogeneity:

1. *develop lower resolution, cost-effective, and fit-for-purpose models that can be built with **limited data at reduced cost**;*
2. *explore subsurface conditions (offshore Gulf of Mexico) that lead to gravitationally stable trapping;*

Motivation

A typical CO_2 storage reservoir:

- Physically and chemically heterogeneous at multiple scales, e.g., lamina, bedding, facies, facies assemblage, formation.
- Site characterization data are not sufficient to resolve small-scale reservoir petrophysical and geochemical variability.
- Reservoir heterogeneity is represented at some “homogenization scale”, e.g.

1. *A facies model was used to simulate CO_2 storage at Sleipner, ignoring sub-facies heterogeneity.*
2. *A formation model was used to evaluate pore pressure from CO_2 injection into the Mt Simon sandstone in Illinois Basin, ignoring heterogeneity within the sandstone.*

- What is the conceptual model uncertainty in CO_2 modeling?
- Is small-scale heterogeneity important for making large-scale long-term predictions?
- Can lower resolution models be useful? And, what are their uses?

We evaluate conceptual models at different resolutions to determine the condition under which low-resolution models can be used to evaluate GCS performance metrics.

Approach

1. Based on a reference heterogeneous model (FHM), create facies models with increasingly reduced *k* resolutions that capture geologic connectivity at different scales.

2. For a range of permeability variances ($\sigma^2_{\ln k}$ = 0.1, 1.0, 4.5)*, compute upscaled *k* for the facies models to reproduce single-phase bulk flow of the FHM, e.g., average fluid pressure and average flow rate.

3. For a range of permeability variances ($\sigma^2_{\ln k}$ = 0.1, 1.0, 4.5), upscale dispersivity for the facies models to reproduce bulk transport of the FHM, e.g., dissolved solute plumes and BTCs.

4. Conduct long-term CO_2 storage simulation using all models. Compare performance metrics: dissolution, CO_2 footprint, CO_2 leakage, reservoir pressure.

**** k ranges from 1 to 6 orders of magnitude;***

Approach

5. Develop, test, and verify a Design of Experiment (DoE) and Response Surface (RS) uncertainty analysis for all models to evaluate:

   1. *If facies models can capture the "parameter space" of the FHM, i.e., key parameters that impact the long-term performance metrics.*

   2. *If facies models can capture the "prediction space" of the FHM, i.e., uncertainty envelope of each performance metric;*

   3. *Determine an optimal facies resolution for each performance metric.*

   4. *Identify a low resolution model for reservoir analysis in lieu of the FHM.*

6. Investigate increasing reservoir depth on storage security: conduct a global sensitivity analysis to evaluate CO_2 storage in GOM sediments.

7. Develop upscaling relations for geochemical parameters of the facies models. Determine optimal resolutions.

Data from the XES facility

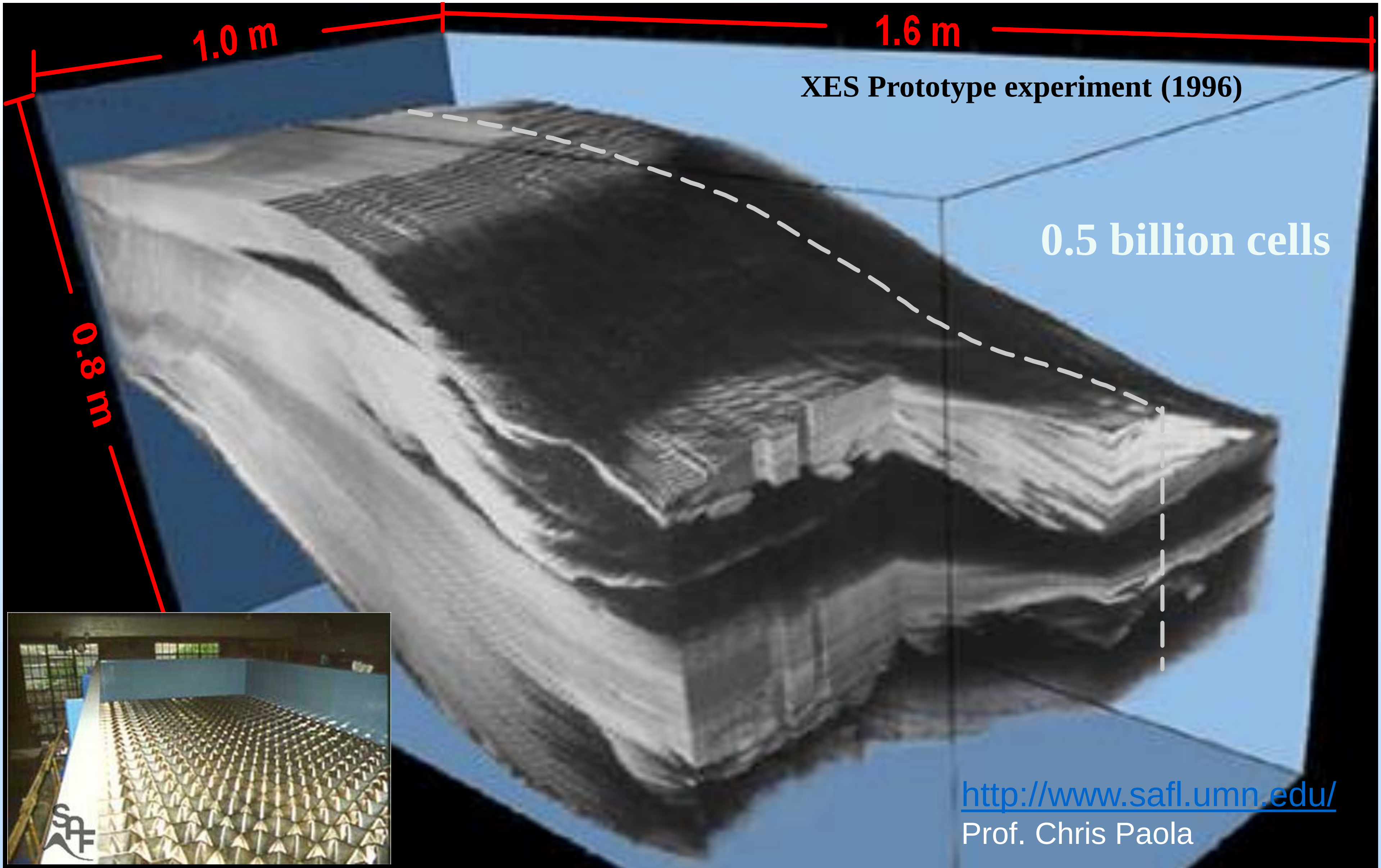

http://www.safl.umn.edu/
Prof. Chris Paola

Conceptual Reservoir Models

Decreasing resolution, decreasing cost →

FHM

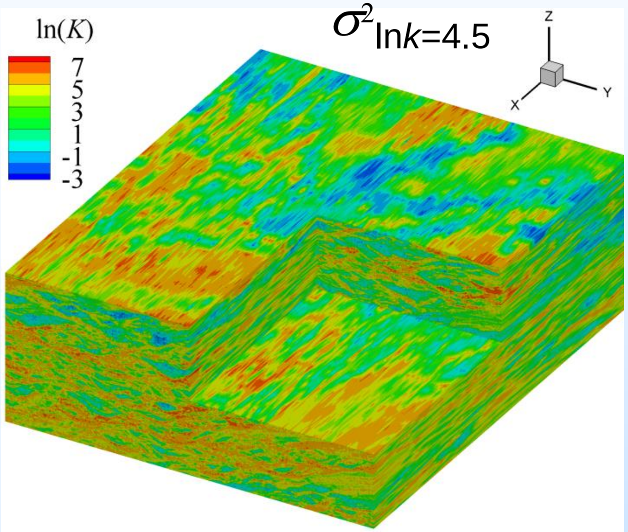

3.2×10^6 individual k values

8-unit facies model

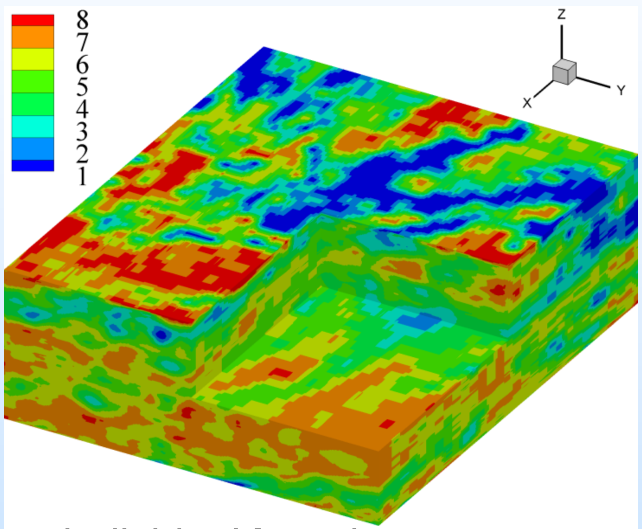

*8 individual **k*** values*

3-unit facies model

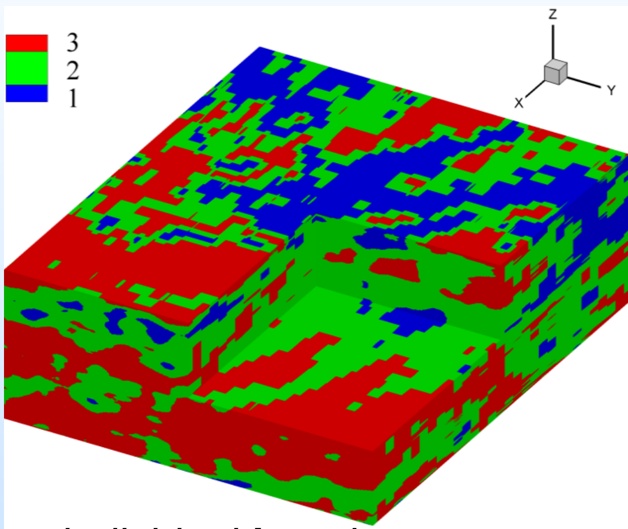

*3 individual **k*** values*

- A 1-unit formation model, where a single ***k**** is computed, is also created.

L_x=5,000 m, L_y=5,000 m, L_z=400 m
N_x=251, N_y=251, N_z=40

Intrinsic Permeability Upscaling

BC$_1$, BC$_2$, …, BC$_m$, Symmetry

$$
\begin{bmatrix}
\left\langle\frac{\partial\Phi}{\partial x}\right\rangle_1 & \left\langle\frac{\partial\Phi}{\partial y}\right\rangle_1 & \left\langle\frac{\partial\Phi}{\partial z}\right\rangle_1 & 0 & 0 & 0 & 0 & 0 & 0 \\
0 & 0 & 0 & \left\langle\frac{\partial\Phi}{\partial x}\right\rangle_1 & \left\langle\frac{\partial\Phi}{\partial y}\right\rangle_1 & \left\langle\frac{\partial\Phi}{\partial z}\right\rangle_1 & 0 & 0 & 0 \\
0 & 0 & 0 & 0 & 0 & 0 & \left\langle\frac{\partial\Phi}{\partial x}\right\rangle_1 & \left\langle\frac{\partial\Phi}{\partial y}\right\rangle_1 & \left\langle\frac{\partial\Phi}{\partial z}\right\rangle_1 \\
\left\langle\frac{\partial\Phi}{\partial x}\right\rangle_2 & \left\langle\frac{\partial\Phi}{\partial y}\right\rangle_2 & \left\langle\frac{\partial\Phi}{\partial z}\right\rangle_2 & 0 & 0 & 0 & 0 & 0 & 0 \\
0 & 0 & 0 & \left\langle\frac{\partial\Phi}{\partial x}\right\rangle_2 & \left\langle\frac{\partial\Phi}{\partial y}\right\rangle_2 & \left\langle\frac{\partial\Phi}{\partial z}\right\rangle_2 & 0 & 0 & 0 \\
0 & 0 & 0 & 0 & 0 & 0 & \left\langle\frac{\partial\Phi}{\partial x}\right\rangle_2 & \left\langle\frac{\partial\Phi}{\partial y}\right\rangle_2 & \left\langle\frac{\partial\Phi}{\partial z}\right\rangle_2 \\
\cdots & \cdots & \cdots & \cdots & \cdots & \cdots & \cdots & \cdots & \cdots \\
\left\langle\frac{\partial\Phi}{\partial x}\right\rangle_m & \left\langle\frac{\partial\Phi}{\partial y}\right\rangle_m & \left\langle\frac{\partial\Phi}{\partial z}\right\rangle_m & 0 & 0 & 0 & 0 & 0 & 0 \\
0 & 0 & 0 & \left\langle\frac{\partial\Phi}{\partial x}\right\rangle_m & \left\langle\frac{\partial\Phi}{\partial y}\right\rangle_m & \left\langle\frac{\partial\Phi}{\partial z}\right\rangle_m & 0 & 0 & 0 \\
0 & 0 & 0 & 0 & 0 & 0 & \left\langle\frac{\partial\Phi}{\partial x}\right\rangle_m & \left\langle\frac{\partial\Phi}{\partial y}\right\rangle_m & \left\langle\frac{\partial\Phi}{\partial z}\right\rangle_m \\
0 & 1 & 0 & -1 & 0 & 0 & 0 & 0 & 0 \\
0 & 0 & 1 & 0 & 0 & 0 & -1 & 0 & 0 \\
0 & 1 & 0 & 0 & 0 & 1 & 0 & -1 & 0
\end{bmatrix}
\cdot
\begin{Bmatrix} k_{xx} \\ k_{xy} \\ k_{xz} \\ k_{yx} \\ k_{yy} \\ k_{yz} \\ k_{zx} \\ k_{zy} \\ k_{zz} \end{Bmatrix}
= (-\mu)
\begin{Bmatrix} \langle q_x\rangle_1 \\ \langle q_y\rangle_1 \\ \langle q_z\rangle_1 \\ \langle q_x\rangle_2 \\ \langle q_y\rangle_2 \\ \langle q_z\rangle_2 \\ \cdots \\ \langle q_x\rangle_m \\ \langle q_y\rangle_m \\ \langle q_z\rangle_m \\ 0 \\ 0 \\ 0 \end{Bmatrix}
$$

Zhang et al. (2006) WRR; Li et al. (2011) WRR

Permeability Upscaling & Verification

- MRE for predicting the single-phase flow rate is similar to MRE for pressure prediction. When ln*k* variance is lower (0.1, 1.0, 4.5), both errors decrease from those of $\sigma^2_{\ln k}$=7.

- For a given $\sigma^2_{\ln k}$, P and flow rate prediction accuracy: 1-unit model < 3-unit model < 8-unit model.

- When $\sigma^2_{\ln k}$ = 7, optimal resolution is the 3-unit model if we accept ~5% error in P and flow rate. If we reduce the error threshold, a higher resolution model (i.e. ,8-unit) is required.

- When $\sigma^2_{\ln k}$ = 0.1, the 1-unit model is optimal for identical error thresholds; When $\sigma^2_{\ln k}$ >>1.0, the 1-unit model is inaccurate: it fails to capture k connectivity which, under high variance, becomes preferential flow.

- **Optimal resolution depends on user-specified error thresholds and the underlying system variability.**

X flow Y flow Z flow

Dispersivity Upscaling & Verification

The plume moments are employed to compare the transport upscaling results as shown in Figure 3. The zero, first and second plume moments are defined as:

$$M=\iiint_{\Omega}(\theta c)dxdydz, \mathbf{L}_p=\frac{1}{M}\iiint_{\Omega}(\mathbf{X}_p\theta c)dxdydz \quad \text{and} \quad s^2=\frac{1}{M}\iiint_{\Omega}(\mathbf{X}_p-\mathbf{L}_p)(\mathbf{X}_p-\mathbf{L}_p)\theta c dxdydz.$$

In addition, both the tailing behavior (Figure 4) and the breakthrough curve (Figure 5) of the FHM have been captured when the variance of ln(*K*) is low to modest.

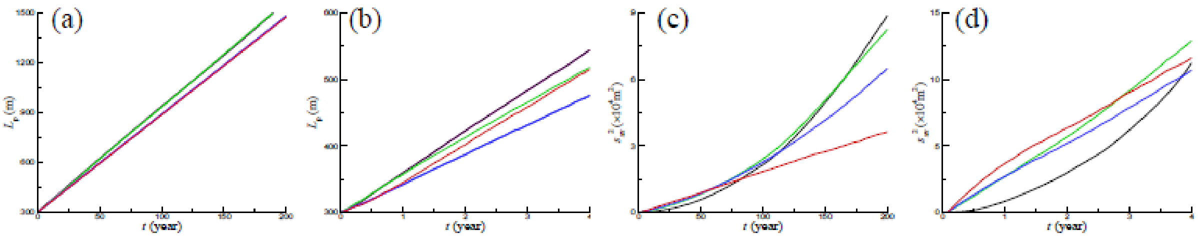

Figure 3. Evolution of plume moments with time: (a) & (b) mean plume displacements for variance(ln*K*) = 0.1 and 4.5, respectively; (c) & (d) longitudinal plume covariances for variance(ln*K*) = 0.1 and 4.5, respectively. The black, red, blue and green lines represent FHM, 1-unit, 3-unit and 8-unit models, respectively.

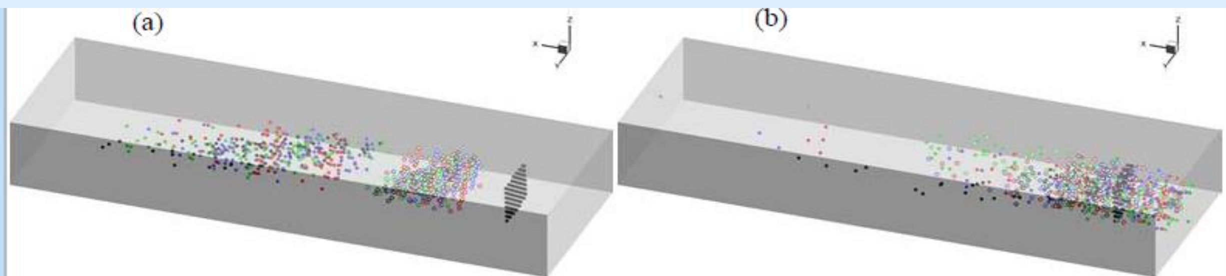

Figure 4. Particle locations in the simulation domain with (a) variance(ln*K*) = 0.1, and (b) variance(ln*K*) = 4.5. The black, red, blue and green points represent particles from the FHM, 1-unit, 3-unit and 8-unit models, respectively. The squares consisting of black points represent initial position. The empty and the filled cycles indicate particles at time 60 years and 180 years for (a) and 1.28 years and 3.84 years for (b). Only 100 particles are shown in one time step.

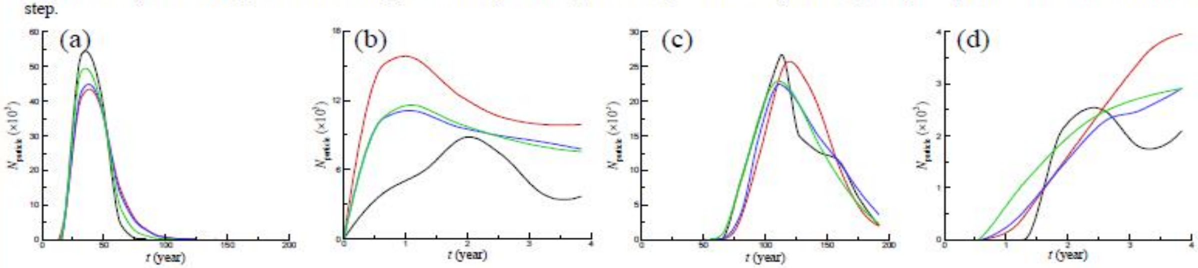

Figure 5. Breakthrough curve: (a) & (b) at *x* = 500m for variance(ln*K*) = 0.1 and 4.5, respectively; (c) & (d) at *x* = 1000m for variance(ln*K*) = 0.1 and 4.5, respectively. The black, red, blue and green lines represent FHM, 1-unit, 3-unit and 8-unit models, respectively.

- For a given variance, accuracy in transport prediction: 8-unit > 3-unit > 1-unit model;
- For $\sigma^2_{\ln k}$ up to 4.5, 8- and 3-unit models can accurately capture the plume migration pathway, mass centroid, and plume dimensions; Optimal resolution: 3-unit model.
- For $\sigma^2_{\ln k} = 0.1$, all models can accurately capture transport BTC; Optimal resolution: 1-unit model.
- For $\sigma^2_{\ln k} = 4.5$, only the 8-unit model can capture some aspects of transport BTC; Optimal resolution: 8-unit or higher.
- ***Solute transport is more sensitive to heterogeneity resolution.*** Optimal resolution depends on the prediction goal and the underlying system variability.

Zhang & Zhang (2016) WRR

CO_2 Storage Modeling

L_x=5,000 m, L_y=5,000 m, L_z=600 m
N_x=251, N_y=251, N_z=60
3.78M grid cells

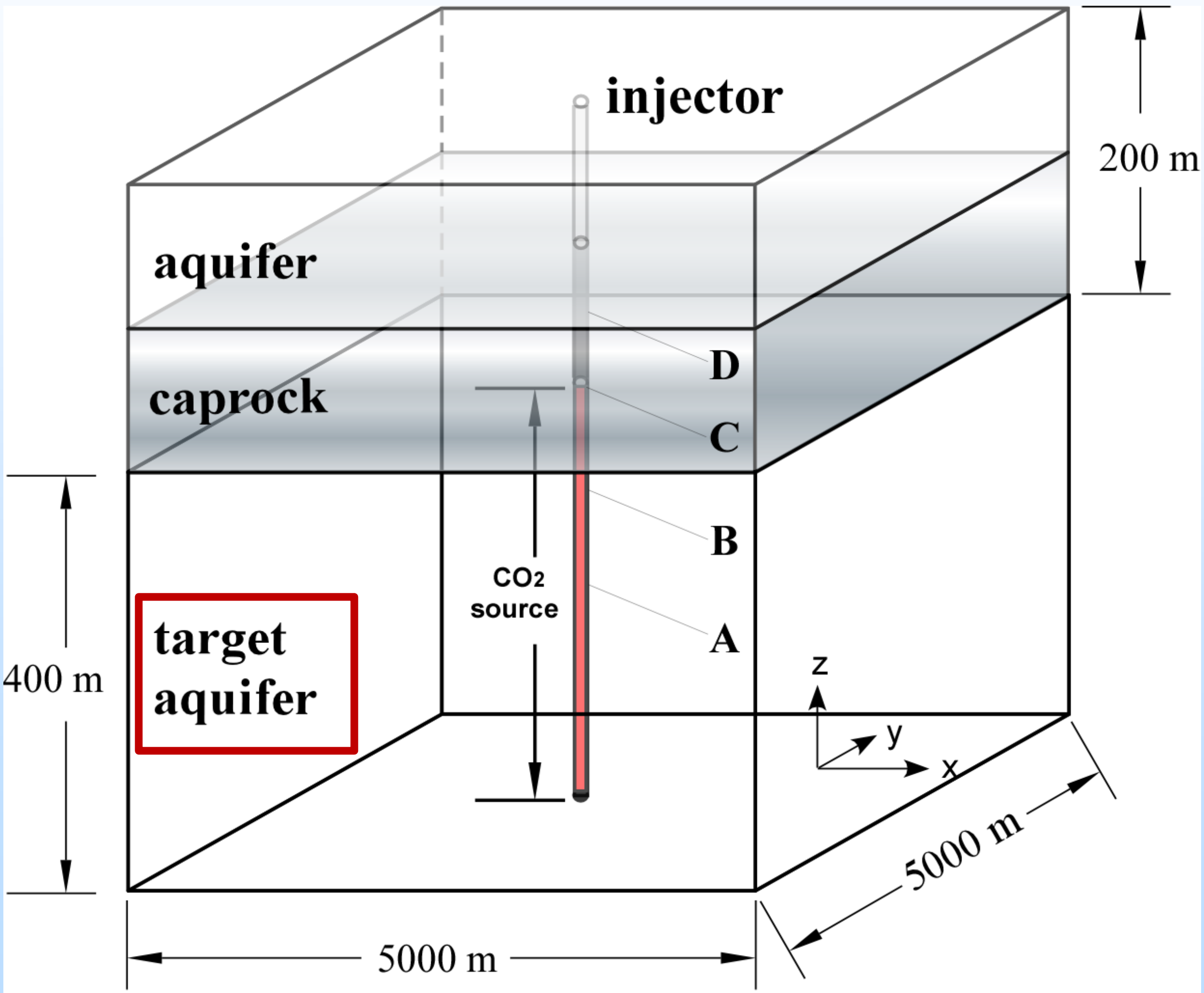

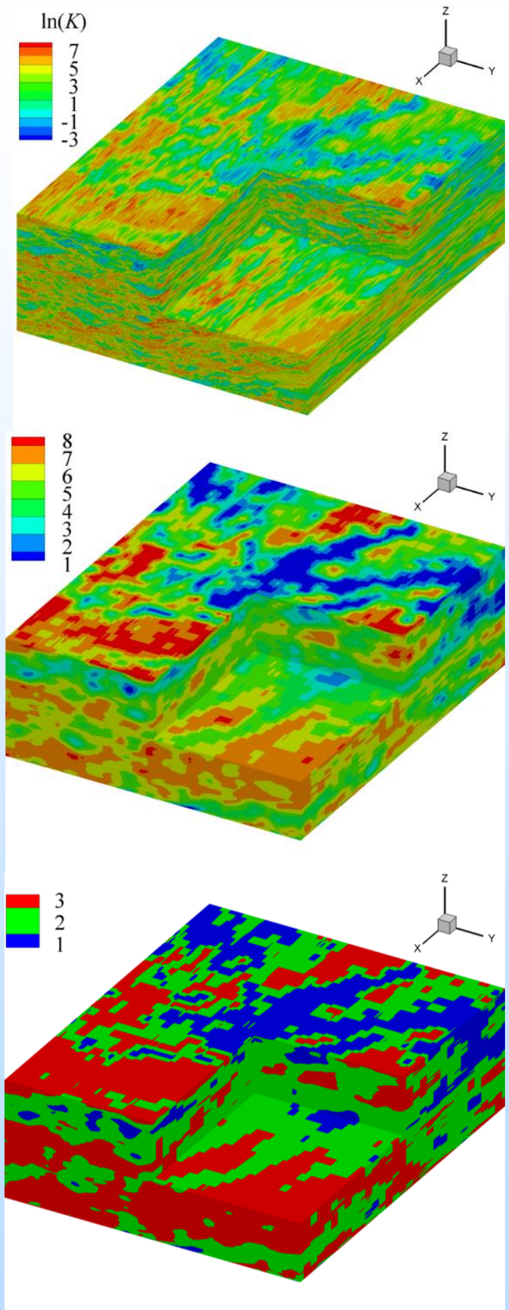

CO_2 Modeling with PFLOTRAN

- Multicomponent-multiphase-multiphysics non-isothermal reactive flow and transport simulator (Multilab open source code: LANL, LBNL, ORNL, PNNL);
- Massively parallel---based on the PETSc parallel framework;
  - Peta-scale performance
  - Highly scalable (run on over 265k cores)
- Supercritical CO_2-H_2O
  - Span-Wagner EOS for CO_2 density & fugacity coefficient
  - Mixture density for dissolved CO_2-brine (Duan et al., 2008)
  - Viscosity CO_2 (Fenghour et al., 1998)
  - P_c assumed zero for viscous (injection) and gravity flow (monitoring);
  - Relative permeability (van Genuchten-Mualem) has no residual trapping;
- Finite Volume Discretization
  - Variable switching for changes in fluid phase
  - Operator splitting for modeling transport and reactions
  - Structured/Unstructured grids
- Object oriented Fortran 2003;
- http://www.pflotran.org/

Performance Scaling on Yellowstone

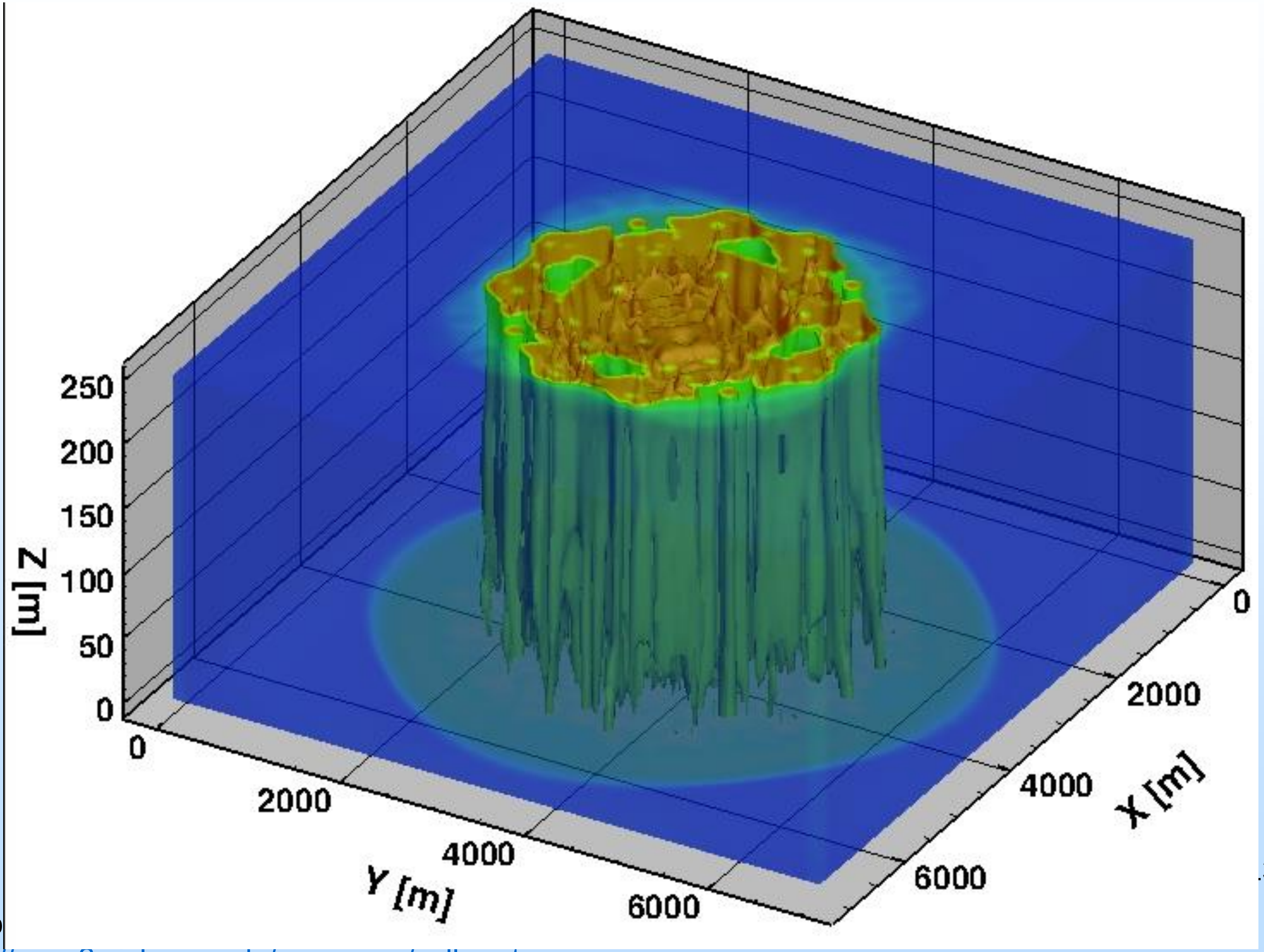

.3

Yello

http://www2.cisl.ucar.edu/resources/yellowstone

Design of Experiment for CO_2 Storage

Case	T Gradient (°C/m)	Brine Salinity (Molal)	k_{cap} (m^2)	Inject rate (kg/s)
1	-0.025	0	$10^{-17.5}$	4
2	-0.025	4	$10^{-17.5}$	4
3	-0.05	0	$10^{-17.5}$	4
4	-0.05	4	$10^{-17.5}$	4
5	-0.0375	2	10^{-16}	2
6	-0.0375	2	10^{-16}	8
7	-0.0375	2	10^{-19}	2
8	-0.0375	2	10^{-19}	8
9	-0.025	2	$10^{-17.5}$	2
10	-0.025	2	$10^{-17.5}$	8
11	-0.05	2	$10^{-17.5}$	2
12	-0.05	2	$10^{-17.5}$	8
13	-0.0375	0	10^{-16}	4
14	-0.0375	0	10^{-19}	4
15	-0.0375	4	10^{-16}	4
16	-0.0375	4	10^{-19}	4
17	-0.025	2	10^{-16}	4
18	-0.025	2	10^{-19}	4
19	-0.05	2	10^{-16}	4
20	-0.05	2	10^{-19}	4
21	-0.0375	0	$10^{-17.5}$	2
22	-0.0375	0	$10^{-17.5}$	8
23	-0.0375	4	$10^{-17.5}$	2
24	-0.0375	4	$10^{-17.5}$	8
25	-0.0375	2	$10^{-17.5}$	4

:ime = 2000 years;

ɪnceptual model in a 3-

*injection rate**

ɪluate their parameter &
ariances (0.1, 1.0, 4.5);

A facies model of the ***lowest*** resolution that can capture the parameter & prediction space of the FHM is considered optimal.

** Injection duration is varied so the same amount of CO_2 is injected.*

Parameter Ranking

Outcome = dissolution storage at 2,000 years

	$\sigma^2 = 0.1$			$\sigma^2 = 1.0$			$\sigma^2 = 4.5$		
Model	Term	Scaled Estimate	Plot Estimate	Term	Scaled Estimate	Plot Estimate	Term	Scaled Estimate	Plot Estimate
1unit	T Gradient	-66525.68		T Gradient	1555.4917		T Gradient	-50947.11	
	Brin Salinity	-17979466		Brin Salinity	-17082310		Brin Salinity	-18280660	
	K Cap	1497108		K Cap	1860613		K Cap	1969252	
	Inj rate	287260.65		Inj rate	241458.07		Inj rate	-104160.2	
3unit	T Gradient	-32093.85		T Gradient	27034.642		T Gradient	17782.292	
	Brin Salinity	-15783477		Brin Salinity	-11537619		Brin Salinity	-9257227	
	K Cap	1460367		K Cap	1767155		K Cap	1770883	
	Inj rate	410148.22		Inj rate	421509.17		Inj rate	-82521.86	
8unit	T Gradient	16158.892		T Gradient	48589.475		T Gradient	60138.433	
	Brin Salinity	-14915585		Brin Salinity	-10880135		Brin Salinity	-8878195	
	K Cap	1776827		K Cap	1745176		K Cap	1735825	
	Inj rate	340980.92		Inj rate	450741.17		Inj rate	426151.34	
FHM	T Gradient	14264.942		T Gradient	39376.7		T Gradient	-6628.533	
	Brin Salinity	-14967318		Brin Salinity	-10393509		Brin Salinity	-8334250	
	K Cap	1765641		K Cap	1687305		K Cap	1611689	
	Inj rate	320034.78		Inj rate	488939.2		Inj rate	544649.55	

Though not capturing the numerical values of the importance statistics of the FHM, all facies models have captured the correct parameter ranking regardless of system *lnk* variance.

For the given ranges of the parameters varied, the most important parameter influencing dissolution storage is salinity.

Parameter Ranking

Outcome = total leakage of CO_2 at 2,000 years

	$\sigma^2 = 0.1$			$\sigma^2 = 1.0$			$\sigma^2 = 4.5$		
Model	Term	Scaled Estimate	Plot Estimate	Term	Scaled Estimate	Plot Estimate	Term	Scaled Estimate	Plot Estimate
1unit	T Gradient	469420.96		T Gradient	-388487.8		T Gradient	-1419857	
	Brin Salinity	-15384250		Brin Salinity	-14242776		Brin Salinity	-8039491	
	K Cap	-76663063		K Cap	73456018		K Cap	81043291	
	Inj rate	-2662427		Inj rate	-3308578		Inj rate	-3977240	
3unit	T Gradient	543991.63		T Gradient	-194952.5		T Gradient	-544753.2	
	Brin Salinity	-18842939		Brin Salinity	-21237658		Brin Salinity	-20641268	
	K Cap	-76407790		K Cap	70965164		K Cap	75600868	
	Inj rate	-2558673		Inj rate	-2872086		Inj rate	-4702174	
8unit	T Gradient	-283710.1		T Gradient	-108156.7		T Gradient	-162012.8	
	Brin Salinity	-19111777		Brin Salinity	-21175701		Brin Salinity	-20683088	
	K Cap	-70108544		K Cap	69845490		K Cap	72073598	
	Inj rate	-2376895		Inj rate	-2710601		Inj rate	-4294708	
FHM	T Gradient	-307085.2		T Gradient	-91501.07		T Gradient	121540.03	
	Brin Salinity	-19035197		Brin Salinity	-20825214		Brin Salinity	-20438426	
	K Cap	-70111854		K Cap	67276691		K Cap	64498465	
	Inj rate	-2453283		Inj rate	-2954034		Inj rate	-3344799	

Though not capturing the numerical values of the importance statistics of the FHM, all facies models have captured the correct parameter ranking regardless of system *lnk* variance.

For the given ranges of the parameters varied, the most important parameter influencing CO_2 leakage is caprock permeability.

Response Surface Modeling (1-Unit; σ^2_{Ink}=0.1)

Outcome= dissolution storage

End of Injection

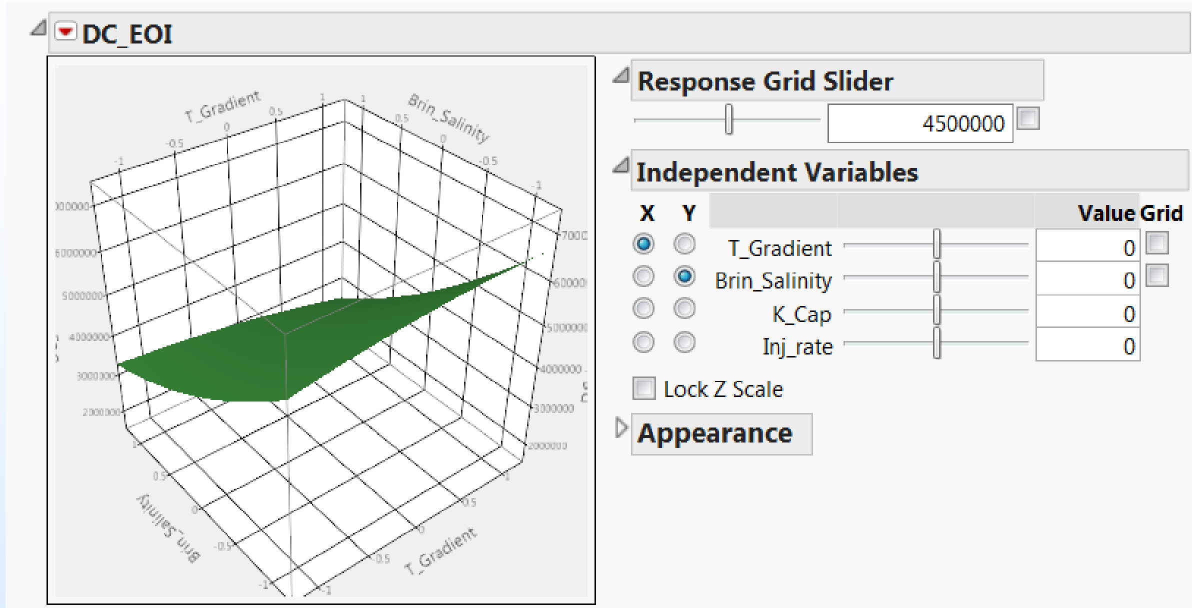

End of Monitoring

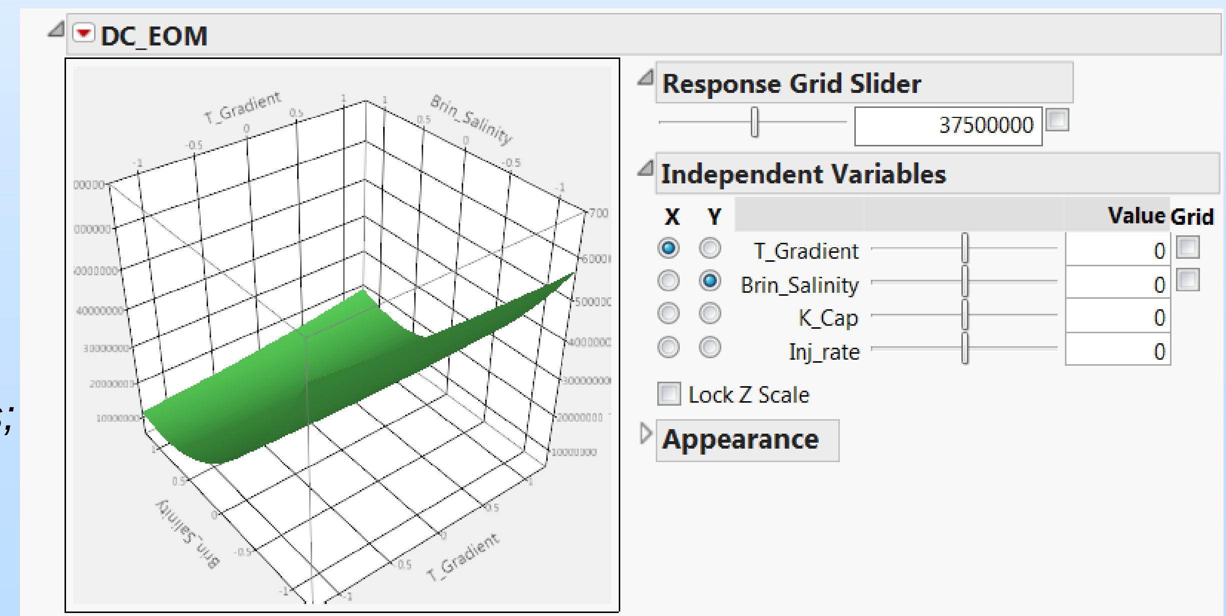

Ongoing work:

- *Create cdf of different predictions at two time scales for all models and for all 3 system variances;*
- *Uncertainty of all predictions using all models will be compared.*

Case 1: isosurface of dissolved CO_2 at 0.004 liquid mole fraction at 2000 years with σ^2 = 0.1 (a - d) and σ^2 = 4.5 (e -h).

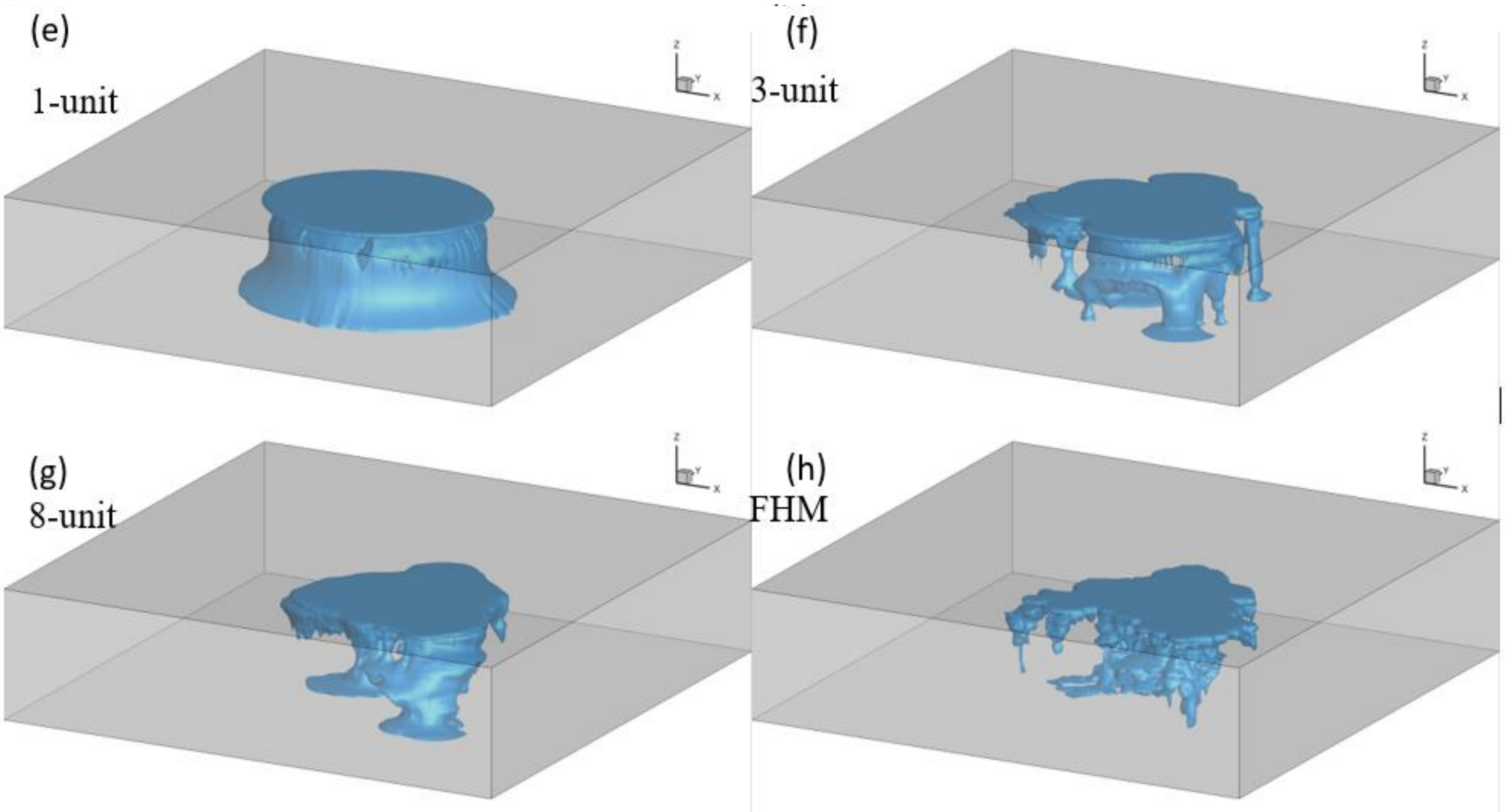

- In the weakly heterogeneous system, convective mixing is simulated by all models.
- In the strongly heterogeneous system (σ^2 =4.5), convective mixing is suppressed by the representation of heterogeneity.

CO_2 dissolution over time for case 2 (high salinity) and case 1 (low salinity):

σ^2 = 0.1 **σ^2 = 1.0** **σ^2 = 4.5**

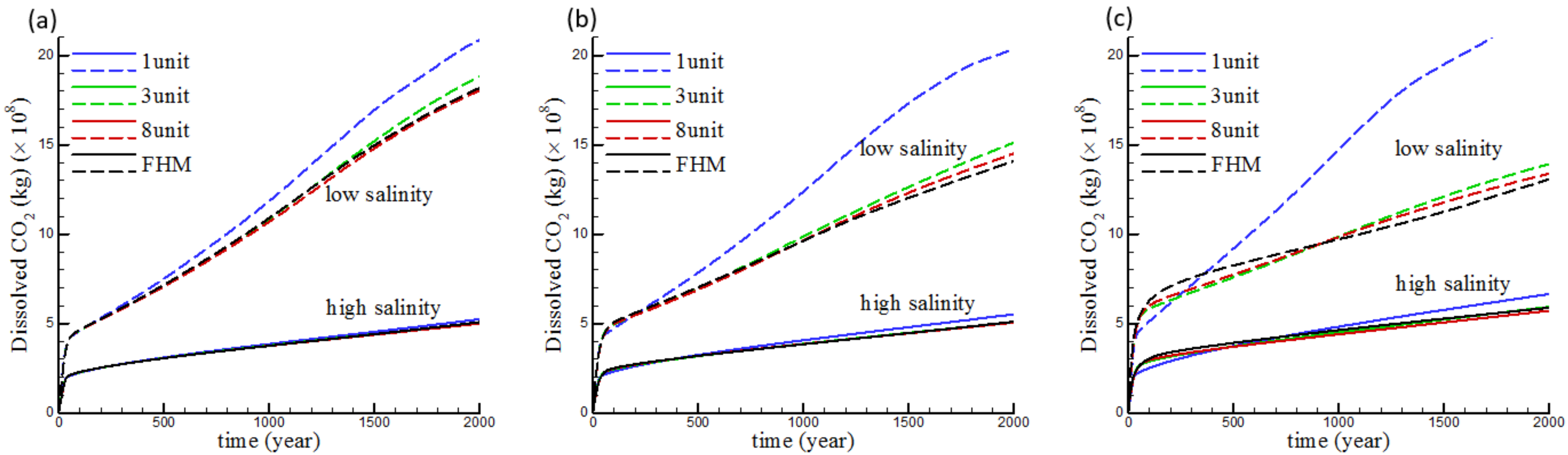

Under high salinity, for all variances, heterogeneity resolution is not important because convective mixing is suppressed: *1-unit model is optimal*.

Under low salinity, for all variances, 1-unit model overestimates dissolution by up to 40% due to enhanced convective mixing; *3-unit model is optimal.*

FHM v. 1-Unit Model Pressure Comparison

$\sigma^2_{\ln k}$=4.5

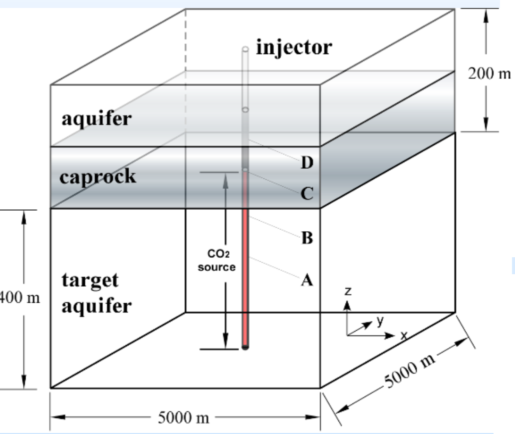

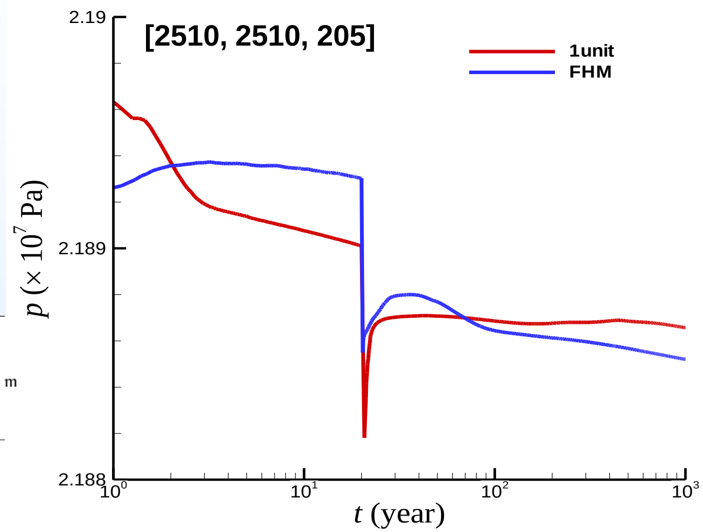

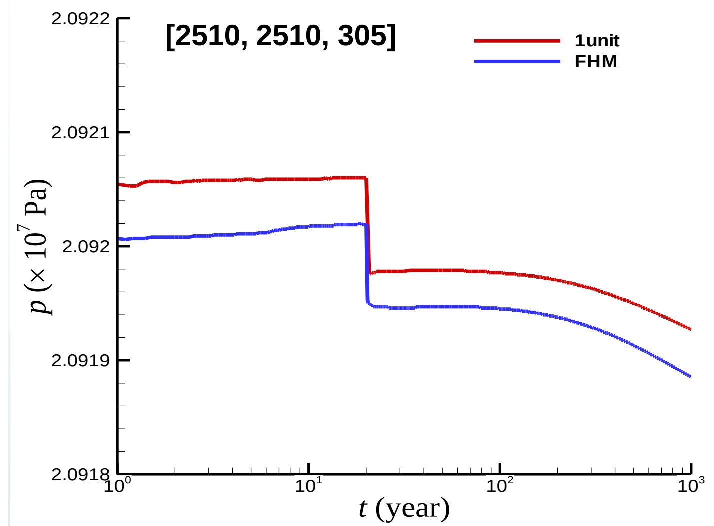

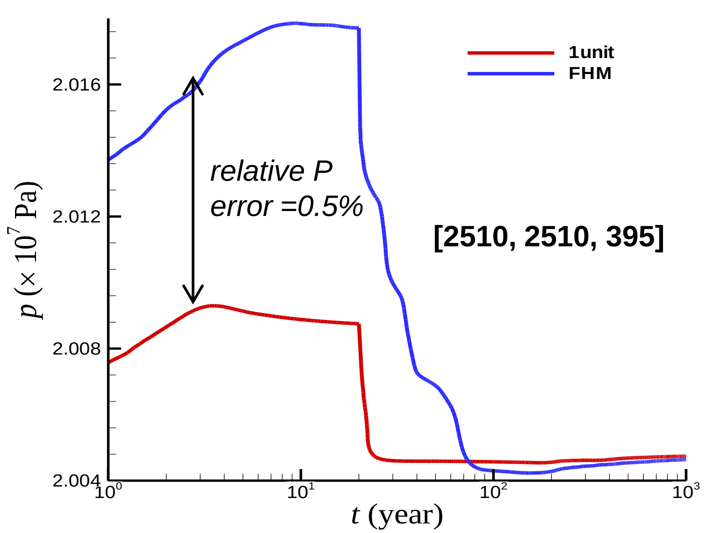

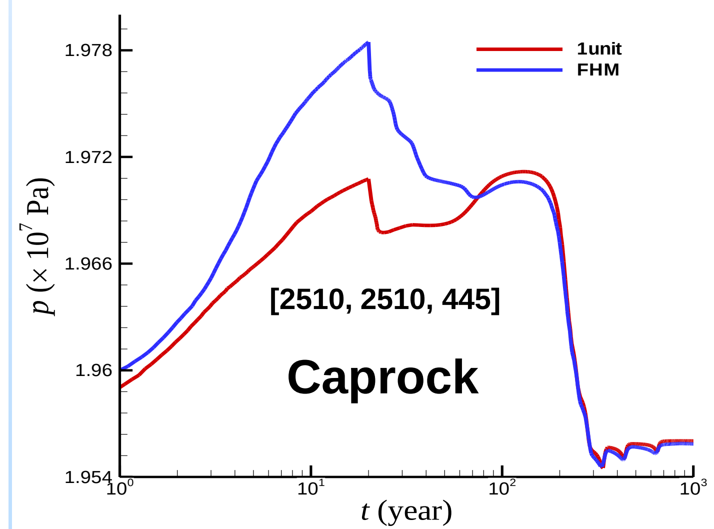

Offshore Storage (Gulf of Mexico)

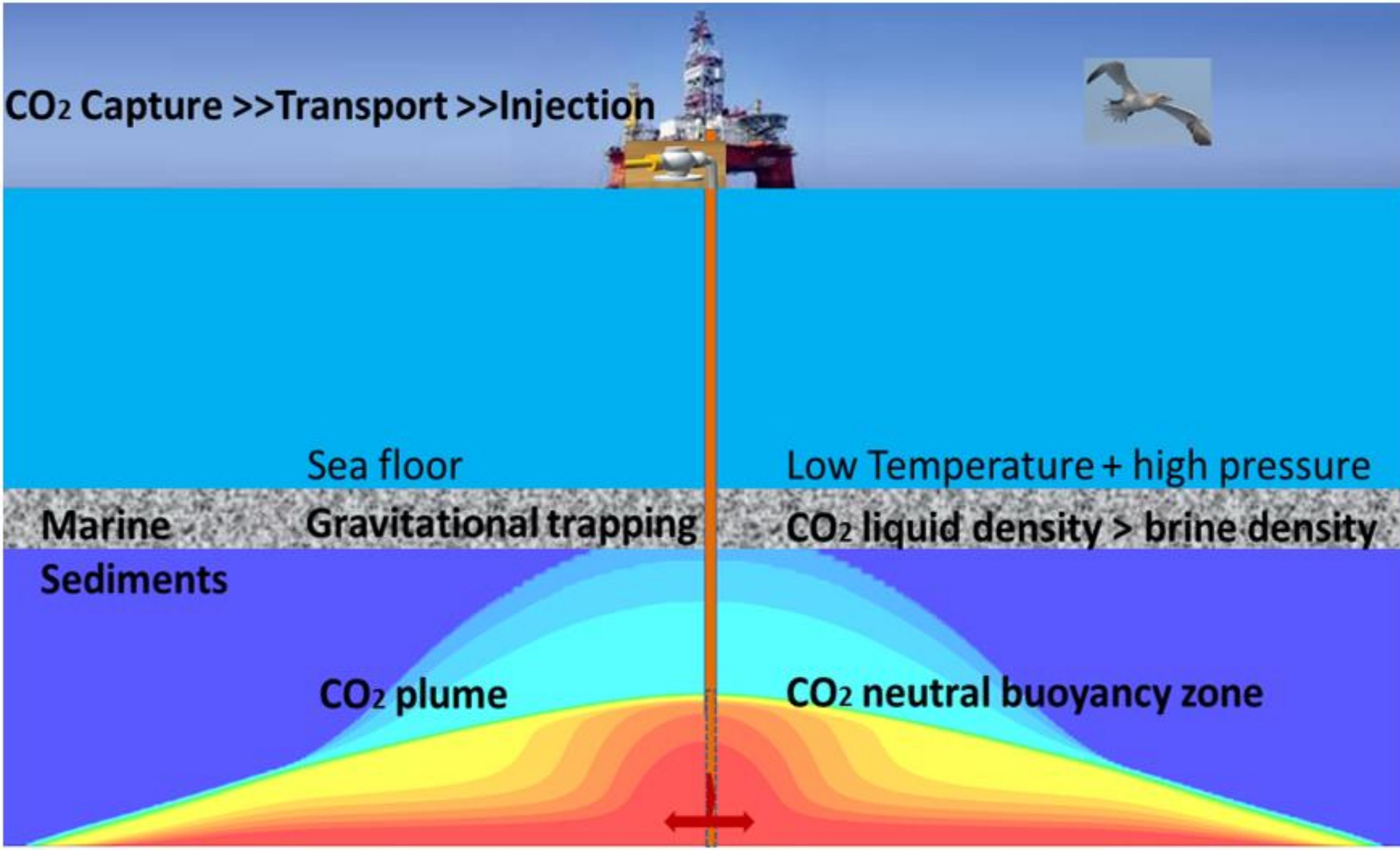

	Uncertain Input parameters*	Min.	Max.	Base case	Distribution
Reservoir Property	Sediment thickness (km)	0.005	0.9	500	Uniform
	Mean permeability (D)	0.001	8	1.0	Log uniform
	Permeability anisotropy factor	0.01	0.5	0.1	Uniform
	Permeability variance	0.0	5.0	0/1.0	Uniform
	Horizontal integral scale (km)	0.5	5.0	1.0	Uniform
	Mean porosity	0.1	0.42	0.2	Correlated to perm
Physical Parameter	**Water depth (km)**	0.1	4.4	2.5	Uniform
	CO_2 injection rate (kg/s)	0.002	2.0	0.3	Correlated to depth
	Seafloor temperature (ºC)	1	20	2	Correlated to depth
	Geothermal gradient (ºC/km)	5	50	20	Correlated to depth

* Based on sediment data collected from 4 GOM sites; temperature and geothermal gradients are from literature. See detail in Dai, Zhang, Stauffer, et al. (2016) Identification of Gravitational Trapping Processes of CO_2 Sequestration in Offshore Marine Sediments, poster presentation, this meeting.

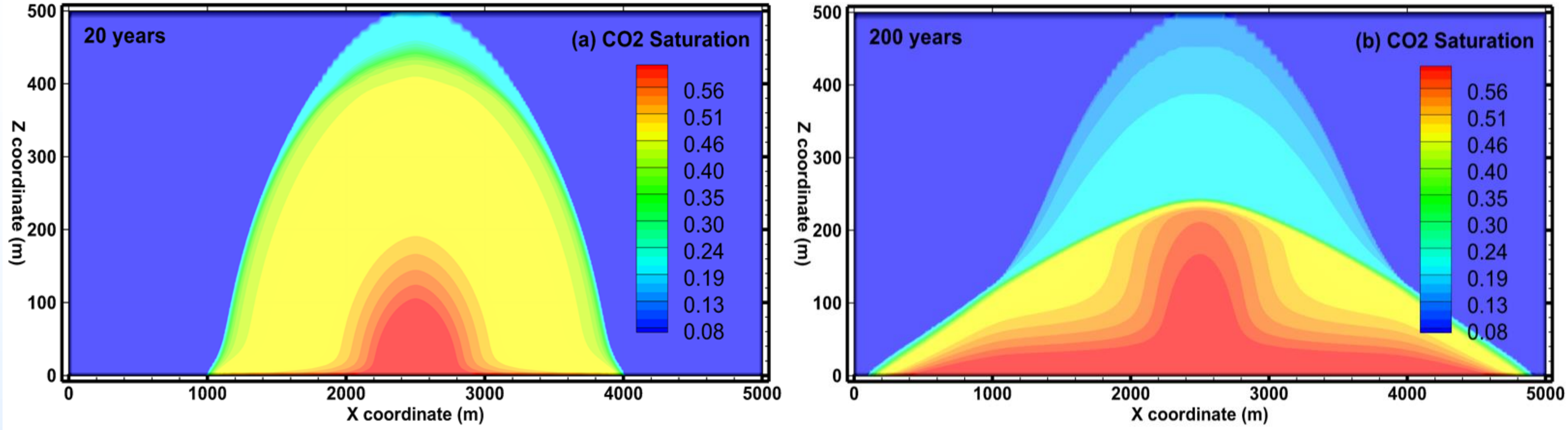

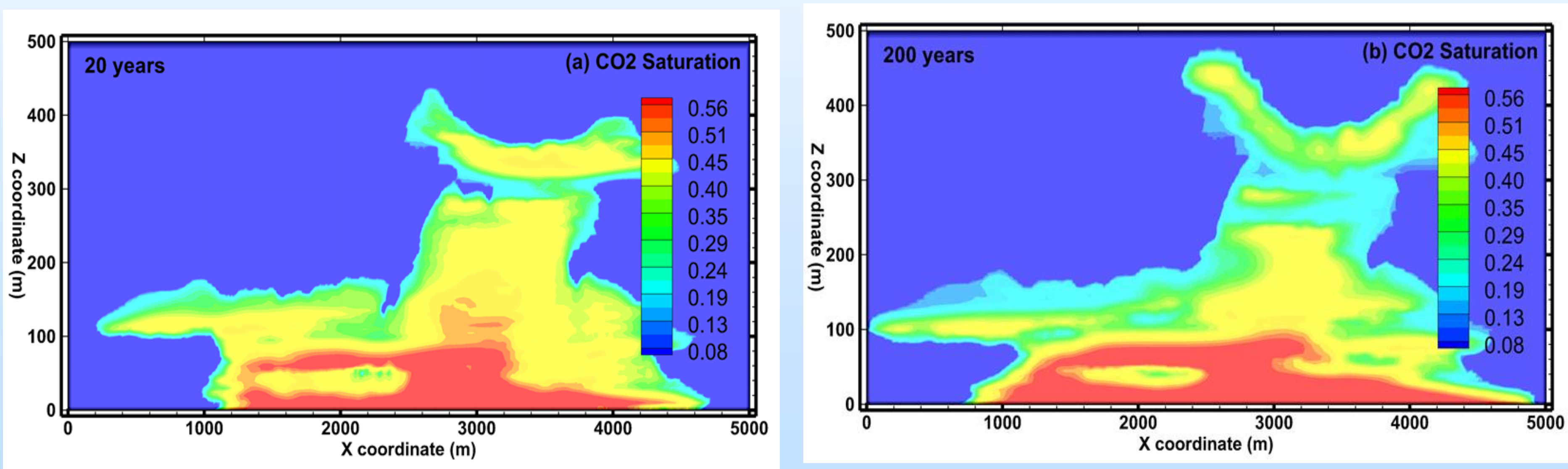

See detail in Dai, Zhang, Stauffer, et. al (2016) Identification of Gravitational Trapping Processes of CO_2 Sequestration in Offshore Marine Sediments, poster presentation, this meeting.

Summary of Progress

- Created high-resolution FHM from an Experimental Stratigraphy; scale it to increasing *lnk* variances (0.1, 1.0, 4.5);
- For each variance, created 3 facies models to with reduced k resolutions;
- Multiscale, multi-variance flow & transport upscaling and verification;
- Multiscale, multi-variance CO_2 storage modeling using PFLOTRAN:
- Under increasing reservoir variability, conduct DoE and RS modeling; evaluate optimal resolution for predicting each performance metric.

(1) scaling on petascale Yellowstone supercomputer at NCAR-Wyoming Supercomputing Center.

*(2) CO_2 simulations and uncertainty analysis have used ~**12 million core hours**.*

- Investigated increasing depth on storage security. Completed a suite of uncertainty analysis using reservoir parameters from the Gulf of Mexico.
- Developed improved geochemical relations for CO_2-fluid-rock reactions.

Key Findings to date

- Permeability upscaling successful for facies models that capture dominant *k* connectivity in three-dimensions. Accuracy of upscaling is affected by system variance & user-specified error threshold;

- For the simulation assumptions employed in this study and for the chosen ranges of the uncertain input parameters:

1. The 1-unit "layer-cake" model is often sufficiently adequate for reproducing pressure & the extent of scCO_2 and dissolved CO_2 footprints, and leakage;

2. The 1-unit model is inaccurate when:

- *salinity is low (convective mixing is overestimated)*
- *strength of heterogeneity is high (preferential flow is not captured);*

3. The 1-unit model preserves the parameter ranking of the FHM for all system variances; 1-unit could be optimal for a parameter sensitivity analysis.

Key Findings to date

4. Dissolution, leakage, footprint, and pressure can be captured by the 3-unit model for all system variances; An overall optimal model.

5. Brine salinity is the single most influential factor impacting dissolution while caprock is the single most influential factor impacting leakage. This finding is independent of the conceptual models and the system variability tested;

- History matching using fluid pressure & plume sizes alone cannot lead to the unique estimation of *k*, as under many conditions, different k parameterizations (8-, 3-, 1-unit) can match these performance metrics equally well. Detailed multiphase saturation and CO_2 breakthrough data are likely needed.

Key Findings to date

Sensitivity analysis with the Gulf of Mexico data:

1. *When lnk variance is high, gravitational trapping can be achieved at a water depth of 1.2 km, extending previously identified self-sealing conditions requiring water depth > 2.7 km.*

2. *Strong permeability/porosity heterogeneity can enhance gravitational trapping.*

Ongoing Research

Our simulation studies have limitations;

Relative permeability upscaling under different capillary, viscosity, versus gravity regimes.

Upscaling of geochemical parameters for the ‘facies’ models;

Develop new reservoir inversion techniques to identify and parameterize facies models without upscaling (Jiao & Zhang, 2016).

Bibliography

- Mingkan Zhang, **Ye Zhang** (2015) Multiscale Dispersivity Upscaling for Three-Dimensional Hierarchical Porous Media, *Water Resources Research*, 51, doi:10.1002/2014WR016202.

- Jianying Jiao, **Ye Zhang** (2016) Direct Method of Hydraulic Conductivity Structure Identification for Subsurface Transport Modeling, *Journal of Hydrologic Engineering*, 10.1061/(ASCE)HE.1943-5584.0001410, 04016033.

- Lichtner, Peter (2016) Kinetic Rate Laws Invariant to Scaling the Mineral Formula Unit, *American Journal of Science*, in press.

- Mingkan Zhang, **Ye Zhang**, Peter Litchtner (2016) Uncertainty analysis in modeling CO2 dissolution in three-dimensional heterogeneous aquifers: effect of multiple conceptual models and explicit fluid flow coupling, *International Journal of Greenhouse Gas Control*, in submission.

- Zhenxue Dai, **Ye Zhang**, Phil Stauffer, Mingkan Zhang, et al. (2016) Identification of gravitational trapping processes of CO_2 sequestration in offshore marine sediments, *Natural Geoscience*, in prep.

Extra Slides

Presentation Outline

– Project Objectives

– Study Approach

– Progress to Date on Key Technical Issues

– Project Wrap-Up

Plans for Remaining Technical Issues

- Complete the geochemical upscaling study to evaluate if HSMs can capture mineral storage when the system contains significant amount of (homogeneous versus heterogeneously distributed) reactive minerals.

- Complete the DoE and RS analysis for all static models with mineral reactions to compare their parameter sensitivity & prediction uncertainty.

- Evaluate the uncertainty in the EOS, which is relevant for identifying suitable conditions for gravity-stable injection in both onshore and offshore settings.

Heterogeneity, Physiochemical Coupling, & Feedback

Base case: No upscaling of geochemical parameters (assume the same bulk mineralogy and reactive mineral parameters):

- How does the resolution of physical heterogeneity affects flow paths and therefore reaction sites and rates and ultimately mineral storage?
- How important is the change in porosity due to the reactions? If important, then feedback between flow and rxn must be accounted for.
- Common assumptions (e.g., Xu et al., 2003, 2004, 2007; Liu et al., 2011; Zhu et al., 2013), neglecting the effect of physical heterogeneity, physiochemical coupling, and (often) porosity-permeability changes and their feedback with flow.

Upscaling mineral specific surface areas

1) Issues linking grain size to FHM's permeability distribution:

- Different published sources reported distinct grain size-permeability relationships for sandstones.
- If any given grain size-permeability relation is used to estimate reactive surface area, the reactive surface areas for different minerals will be the same, which is not consistent with detailed laboratory measurements reported in the literature.

2) Issues using surface roughness to distinguish different minerals:

- The calculated reactive surface area using surface roughness is several orders of magnitude different from the experiment data from the literature.

3) Issues using an empirical formula directly linking grain size to reactive surface area:

Grain size is no longer a constant value compared to experiment data from the literature. Therefore, we have to measure grain size for every mineral.

4) Issues using an empirical formula directly linking reactive surface area to *lnk*:

High uncertainty (ranging form positive, zero, to negative) exists in their correlation.

Parallel Simulation for k Upscaling

Test model (0.4M):

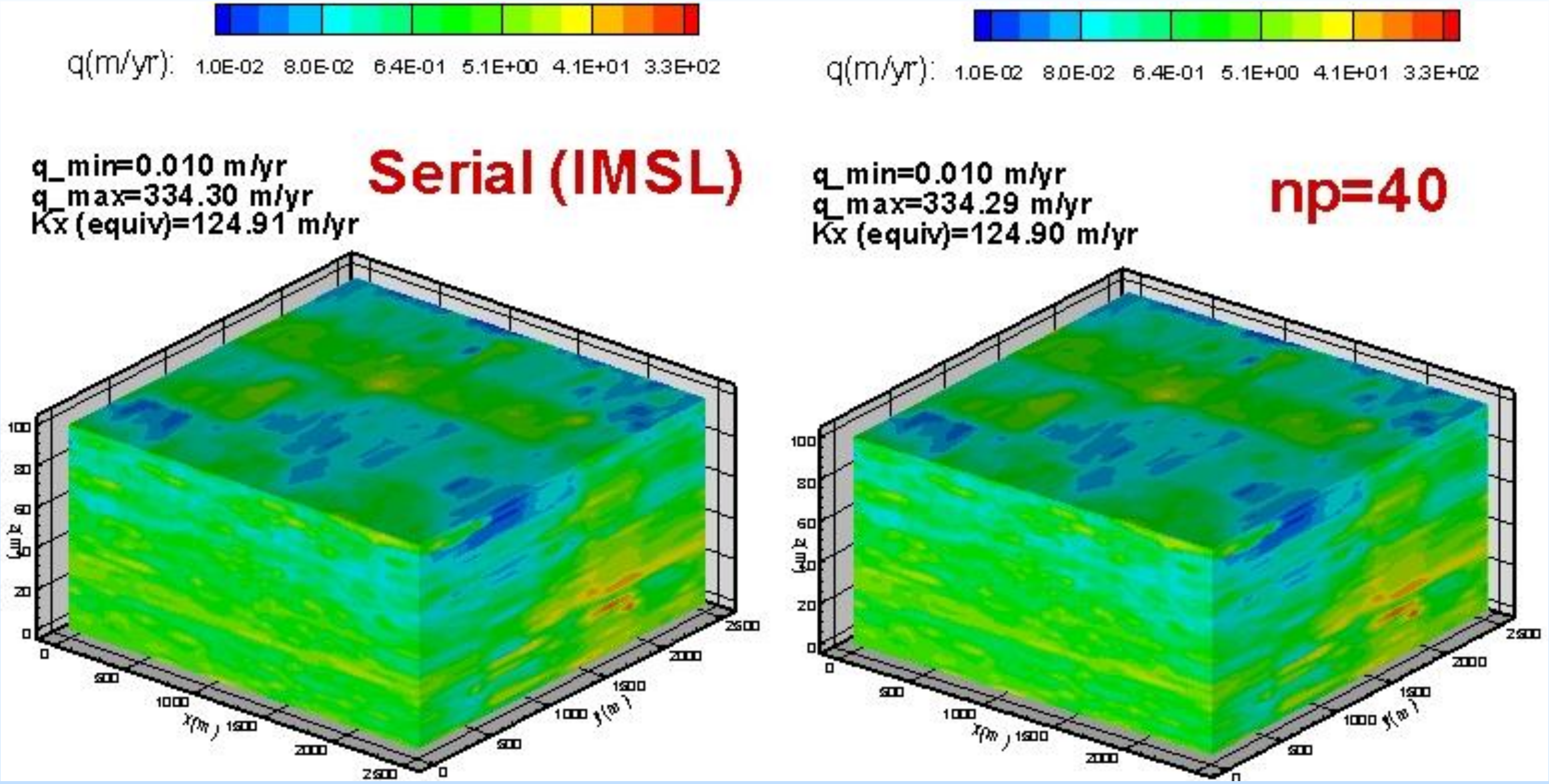

Serial time (calling an optimized IMSL on BigRed at IU): 1 hour

Parallel time (H2oc.gg.uwyo.edu): 37 sec (64 processors)

PFLOTRAN formulations

To model GCS, the following mass and energy conservation equations are solved:

$$\frac{\partial}{\partial t}\left[\varphi \sum_{\alpha} (\rho_\alpha s_\alpha X_i^\alpha)\right] + \nabla \cdot \sum_{\alpha} (\rho_\alpha X_i^\alpha \vec{q}_\alpha - \varphi \rho_\alpha s_\alpha \tau_\alpha D_\alpha \nabla X_i^\alpha) = S_i \qquad (1)$$

$$\frac{\partial}{\partial t}\left[\varphi \sum_{\alpha} (\rho_\alpha s_\alpha U_\alpha) + (1-\varphi)\rho_r C_{p,r} T\right] + \nabla \cdot \left[\sum_{\alpha} (\vec{q}_\alpha \rho_\alpha H_\alpha) - \lambda \nabla T\right] = Q \qquad (2)$$

φ denotes porosity, and $\rho_\alpha, s_\alpha, \tau_\alpha, D_\alpha, U_\alpha, H_\alpha$ refer to the density, saturation, tortuosity, diffusion coefficient, internal energy, and enthalpy of fluid phase α, respectively. Two fluid phases (CO_2, brine) will be modeled. The quantities X_i^α denote the mole fraction of component *i* in phase α. The quantities $C_{p,r}$ and λ denote the rock heat capacity and conductivity, respectively. The summation is carried out over all fluid phases present in the system. The system is assumed locally to be in thermodynamic equilibrium with temperature $T(\vec{x};t)$ at position $\vec{x}$ and time *t*. The quantity *Q* denotes an energy source/sink term.

The quantity *Si* denotes a source/sink term for the *i*th primary species describing reaction with minerals given by $S_i = -\sum_m \nu_{im} I_m$, with stoichiometric reaction coefficients ν_{im} and kinetic rate I_m for the *m*th mineral, taken as positive for precipitation and negative for dissolution.

The flow rate $\vec{q}_\alpha$ of fluid phase α is given by the extended Darcy's law: $\vec{q}_\alpha = -\frac{\bar{\bar{k}} k_\alpha}{\mu_\alpha}(\nabla p_\alpha - \rho_\alpha g z)$, with intrinsic permeability $\bar{\bar{k}}$, relative permeability k_α, fluid viscosity μ_α, and pressure p_α of phase α.

Code Comparison with TOUTHREACT

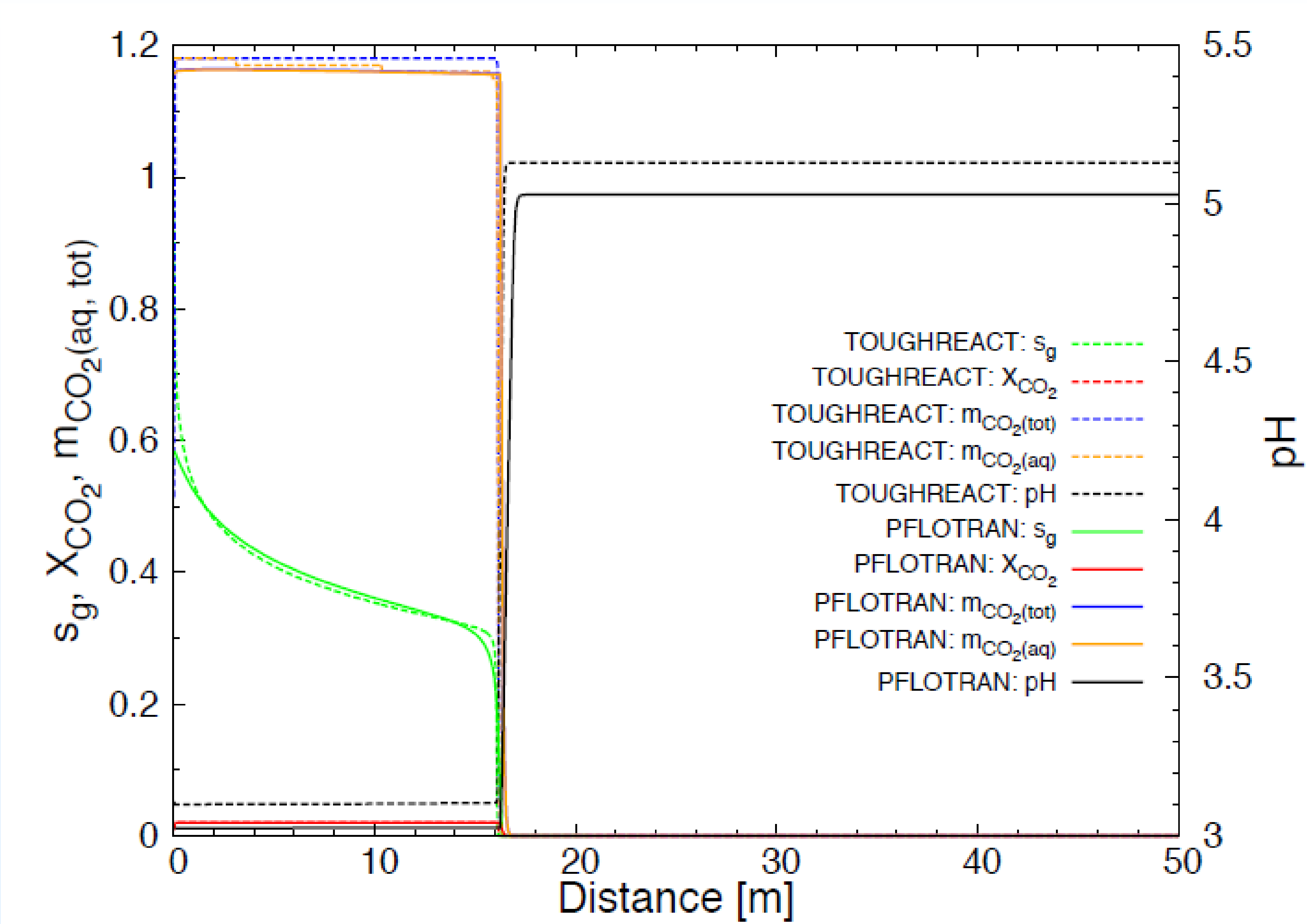

Uncertainty Factors

Uncertainty factors evaluated for the reactive mineral end-members:

1. keff of Chlorite (Chl_keff)
2. abundance of Chlorite (Chl_Abund),
3. keff of plagioclase (Plag_Keff),
4. abundance of plagioclase (Plag_Abund),
5. Geochemical database.

Uncertainty Factors

Uncertainty factors evaluated for the fast-reacting mineral end-members:

1. keff of Chlorite (Chl_keff)
2. abundance of Chlorite (Chl_Abund),
3. keff of plagioclase (Plag_Keff),
4. abundance of plagioclase (Plag_Abund),
5. Database.

	Chl_Keff	Chl_Abund	Plag_Keff	Plag_Abund	Database
1	0	0	-1	0	L2
2	-1	1	-1	-1	L2
3	0	0	0	0	L2
4	0	1	0	0	L1
5	1	1	-1	1	L2
6	0	-1	-1	1	L1
7	1	-1	0	0	L1
8	0	0	0	-1	L2
9	-1	0	-1	-1	L1
10	1	-1	-1	-1	L2
11	-1	-1	1	1	L1
12	1	-1	1	1	L2
13	-1	1	-1	1	L1
14	1	0	1	-1	L1
15	-1	-1	0	1	L2
16	-1	0	0	0	L1
17	-1	1	1	-1	L1
18	1	0	0	1	L1
19	1	1	1	-1	L2
20	0	1	1	1	L1
21	-1	1	1	1	L2
22	1	1	-1	-1	L1
23	-1	-1	-1	0	L2
24	-1	-1	1	-1	L2
25	0	-1	0	-1	L1
26	0	0	1	0	L2

Changes in Volume Fraction:

Chlorite after 2000 years

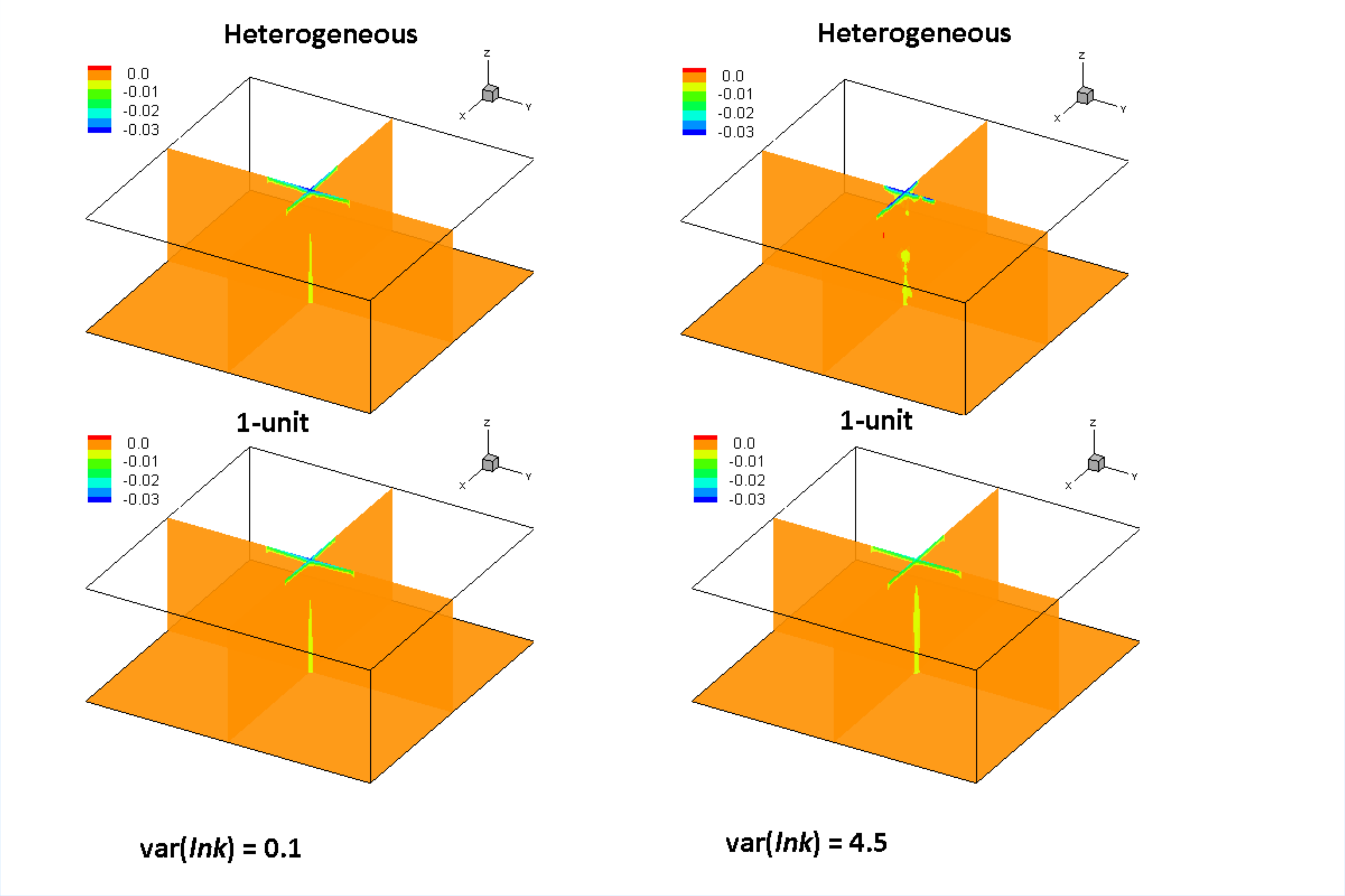

Changes Volume Fraction: Siderite after 2000 years

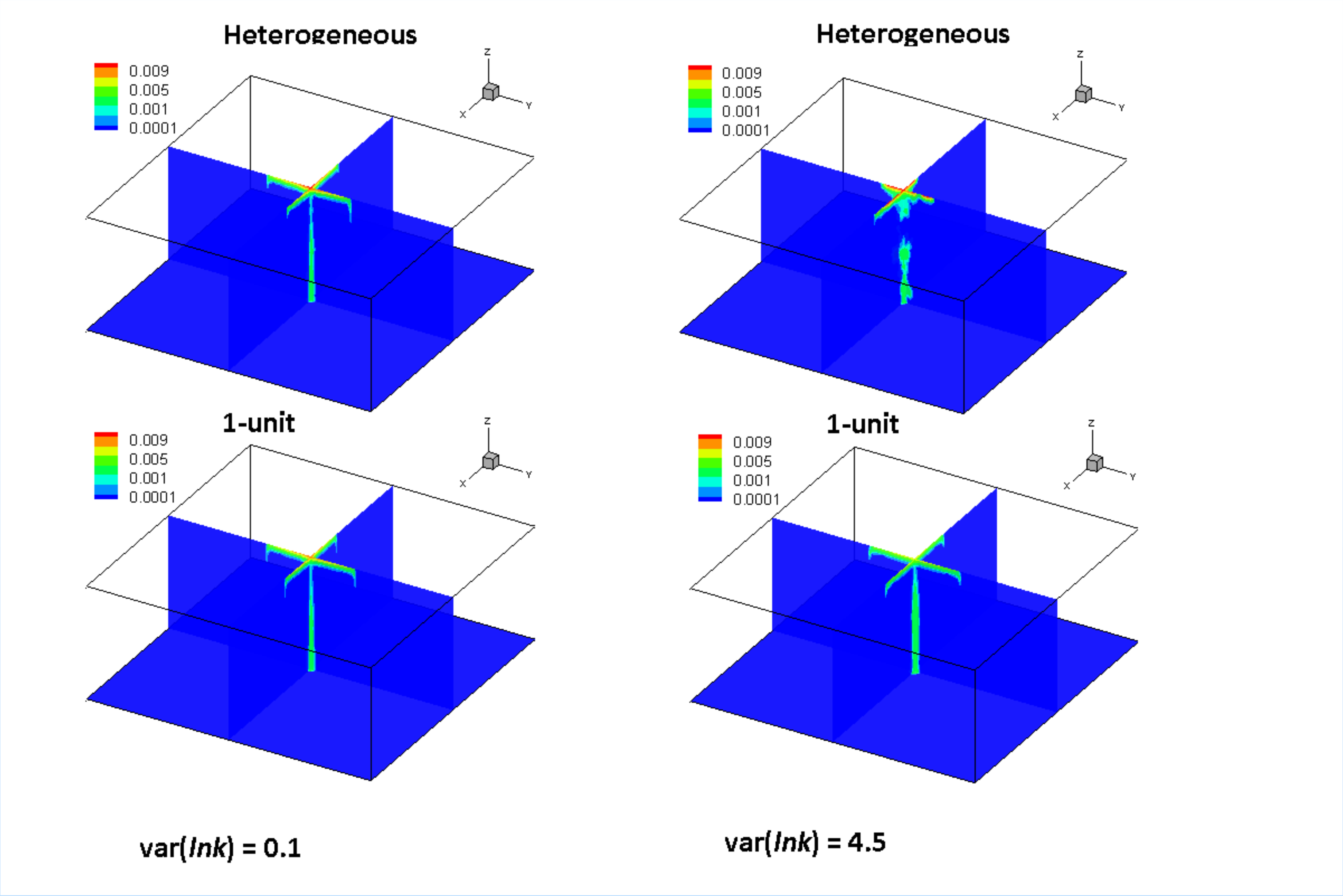

Changes Volume Fraction: Magnesite after 2000 years

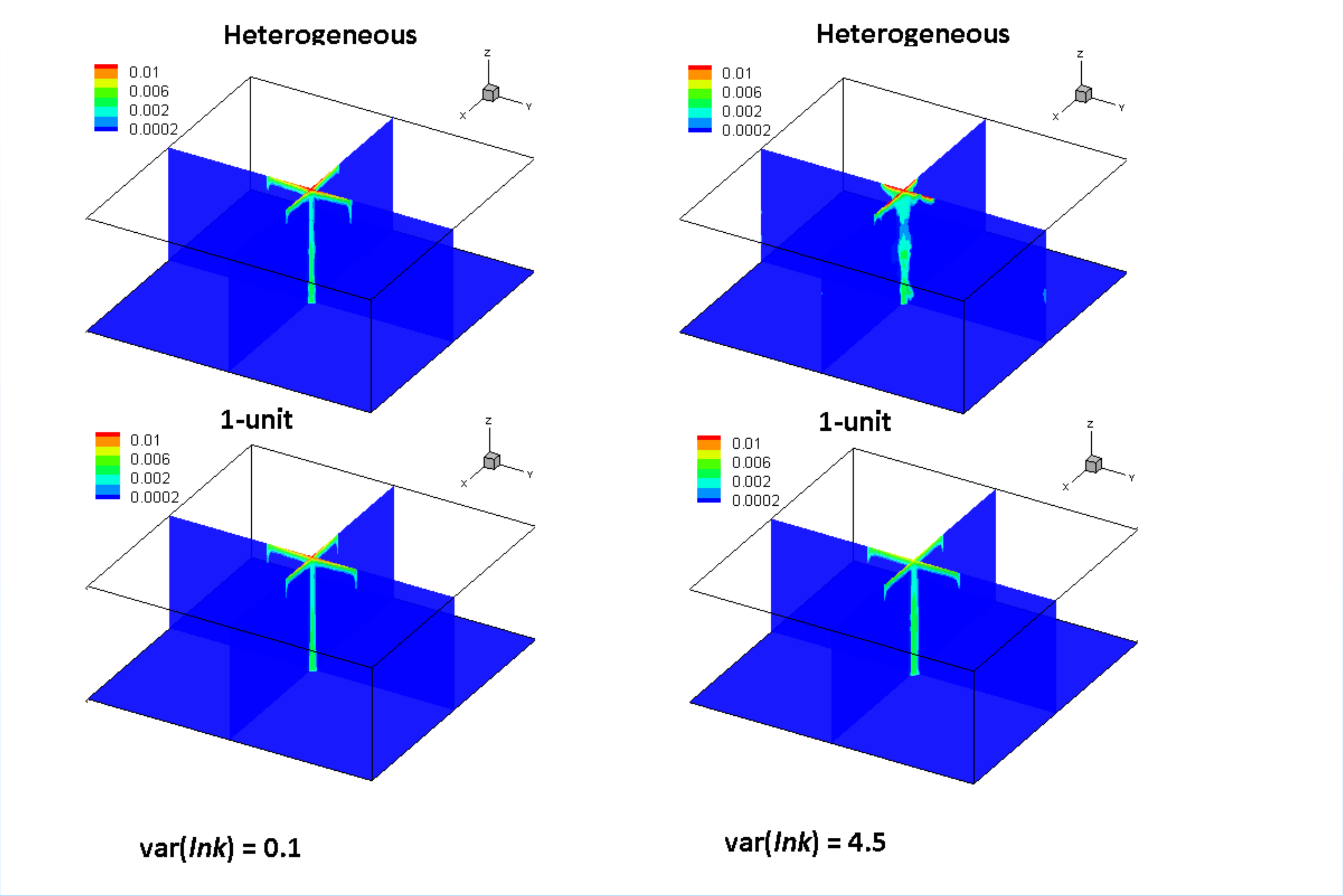

Changes Volume Fraction: without Chlorite after 2000 years

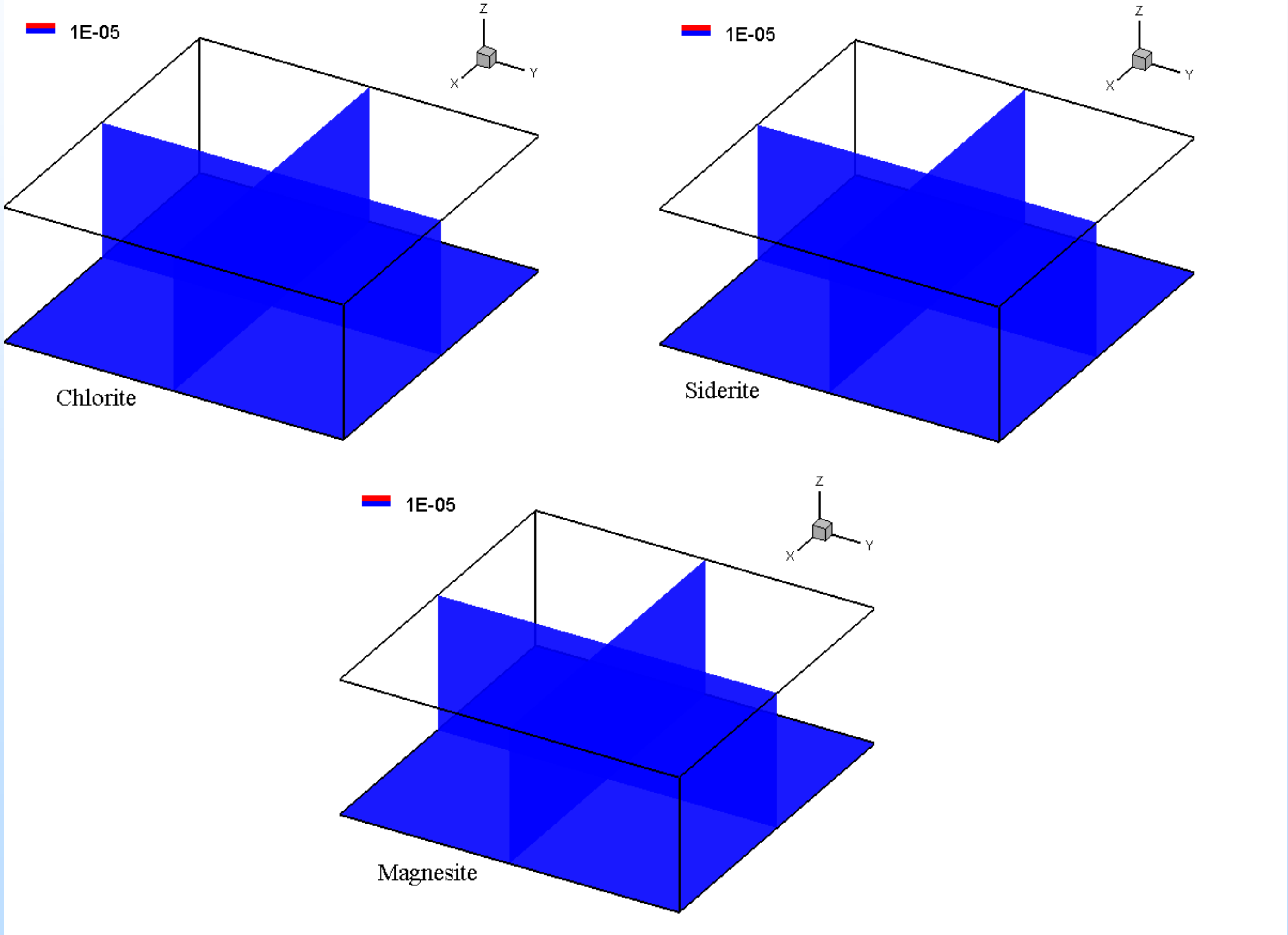

	Chl_Keff	Chl_Abund	Plag_Keff	Plag_Abund	Database
1	0	0	-1	0	L2
2	-1	1	-1	-1	L2
3	0	0	0	0	L2
4	0	1	0	0	L1
5	1	1	-1	1	L2
6	0	-1	-1	1	L1
7	1	-1	0	0	L1
8	0	0	0	-1	L2
9	-1	0	-1	-1	L1
10	1	-1	-1	-1	L2
11	-1	-1	1	1	L1
12	1	-1	1	1	L2
13	-1	1	-1	1	L1
14	1	0	1	-1	L1
15	-1	-1	0	1	L2
16	-1	0	0	0	L1
17	-1	1	1	-1	L1
18	1	0	0	1	L1
19	1	1	1	-1	L2
20	0	1	1	1	L1
21	-1	1	1	1	L2
22	1	1	-1	-1	L1
23	-1	-1	-1	0	L2
24	-1	-1	1	-1	L2
25	0	-1	0	-1	L1
26	0	0	1	0	L2

Changes in Volume Fraction:

Chlorite after 2000 years

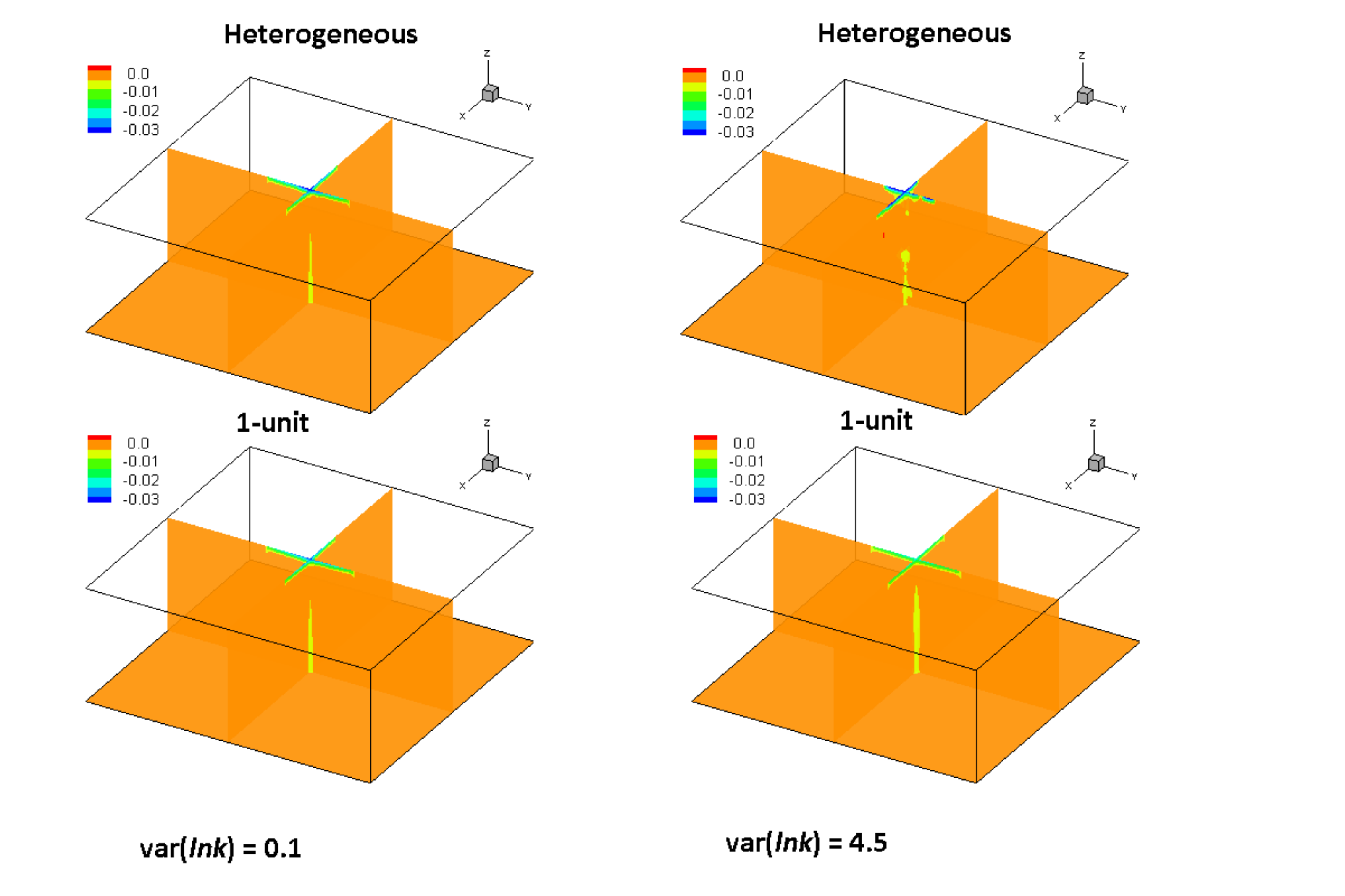

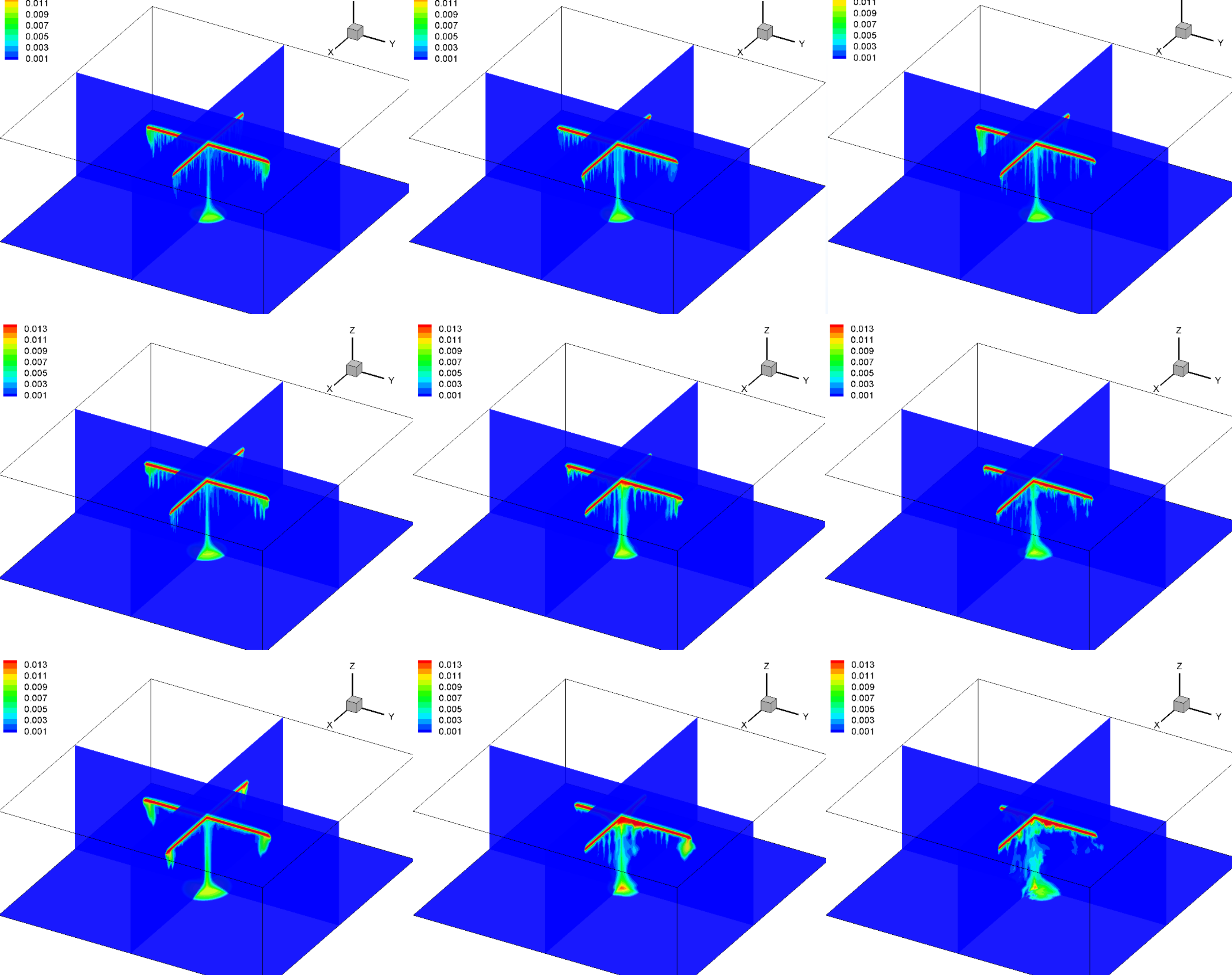
0.011
0.009
0.007
0.005
0.003
0.001
X
Y
0.011
0.009
0.007
0.005
0.003
0.001
X
Y
0.011
0.009
0.007
0.005
0.003
0.001
X
Y
0.013
0.011
0.009
0.007
0.005
0.003
0.001
Z
X
Y
0.013
0.011
0.009
0.007
0.005
0.003
0.001
Z
X
Y
0.013
0.011
0.009
0.007
0.005
0.003
0.001
Z
X
Y
0.013
0.011
0.009
0.007
0.005
0.003
0.001
Z
X
Y
0.013
0.011
0.009
0.007
0.005
0.003
0.001
Z
X
Y
0.013
0.011
0.009
0.007
0.005
0.003
0.001
Z
X
Y

FHM v. 1-Unit Model

(An identical set of DoE dynamic parameters)

Dissolved CO_2 at the end of monitoring (inj rate= 0.05 Mt/yr):

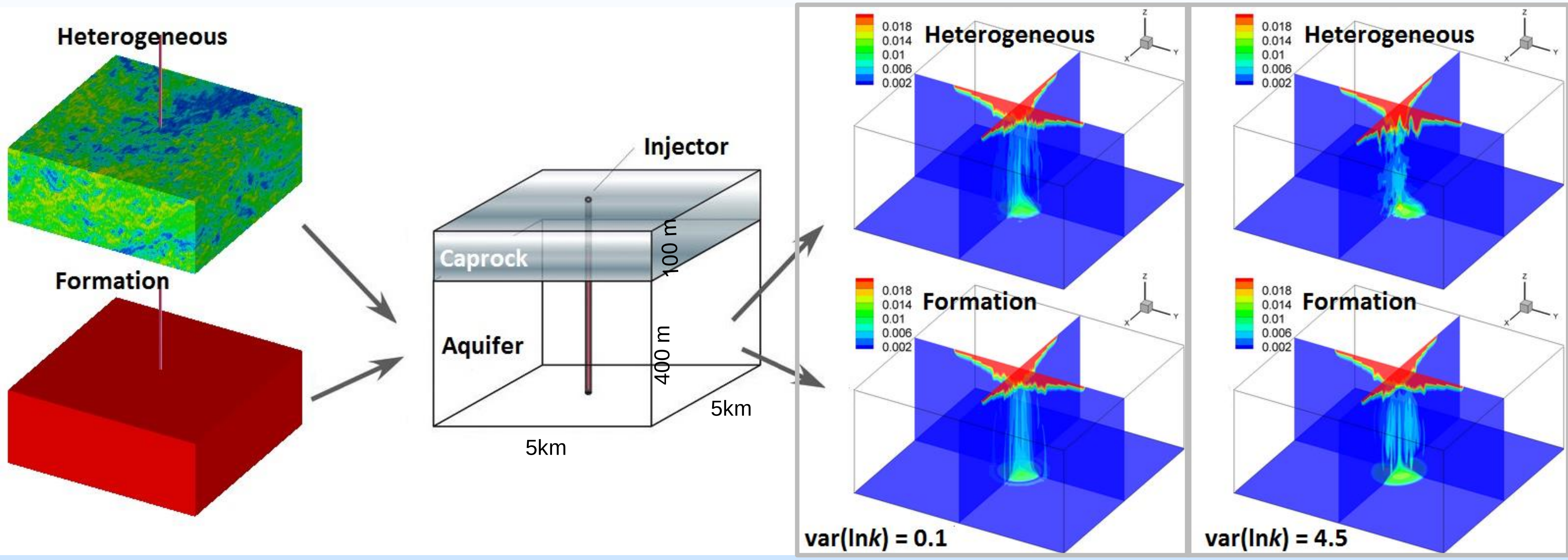

Under both low and high variances, for the given combination of dynamic parameters, the 1-unit model can capture plume footprint and fluid pressure distribution of the FHM well. For these performance metrics, 1-unit model is sufficient, even though the 8-unit and 3-unit models yield more accurate predictions (not shown);

FHM v. HSMs (Dissolved CO_2 plume)

(An identical set of DoE dynamic parameters)

Dissolved CO_2 at the end of monitoring (inj rate= 0.063 Mt/yr):

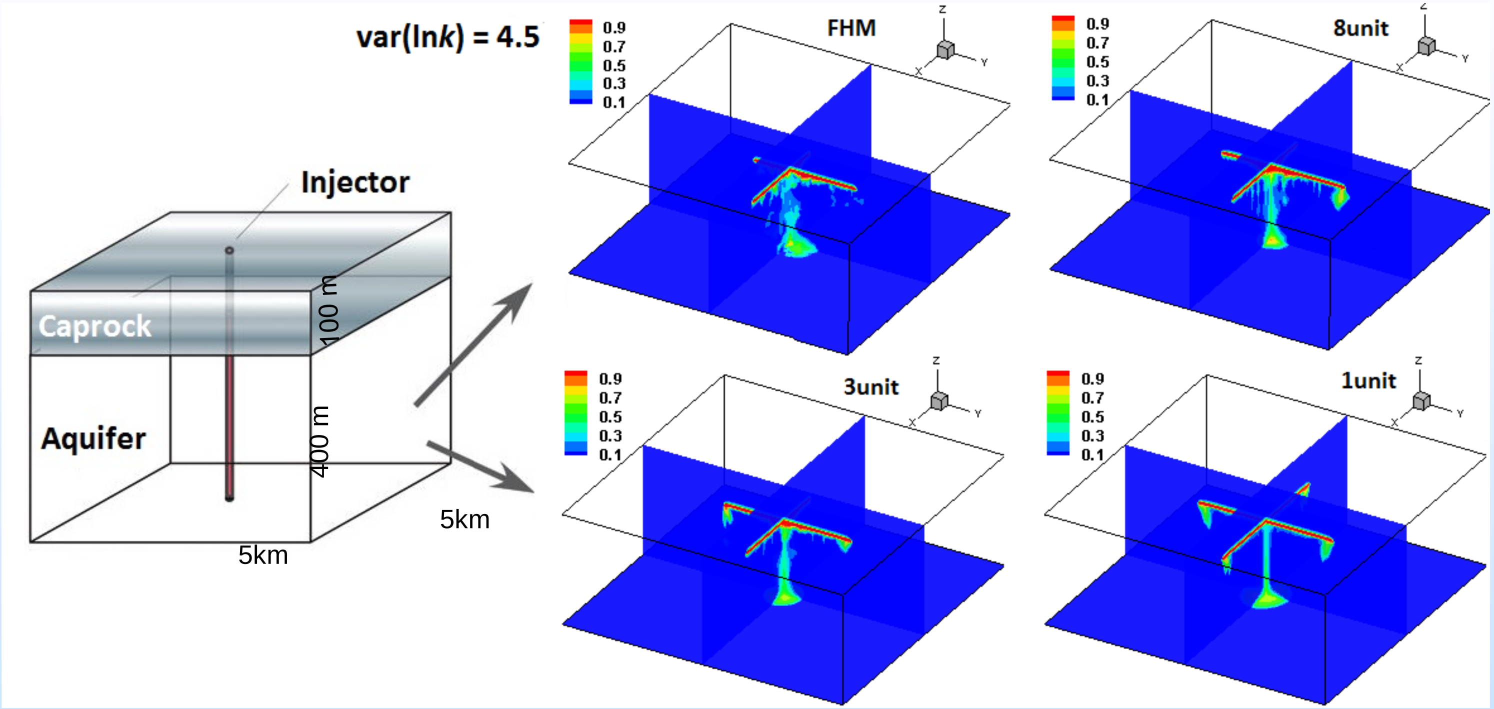

Under high reservoir lnk variances, for the given combination of dynamic parameters, the 1-unit model can capture $scCO_2$ plume footprint and fluid pressure distribution of the FHM well. For these performance metrics, 1-unit model is sufficient, even though the 8-unit and 3-unit models yield more accurate predictions (not shown);

FHM v. 1-Unit Model (Dissolved CO_2 Plume)

(An identical set of DoE dynamic parameters)

Dissolved CO_2 at the end of monitoring

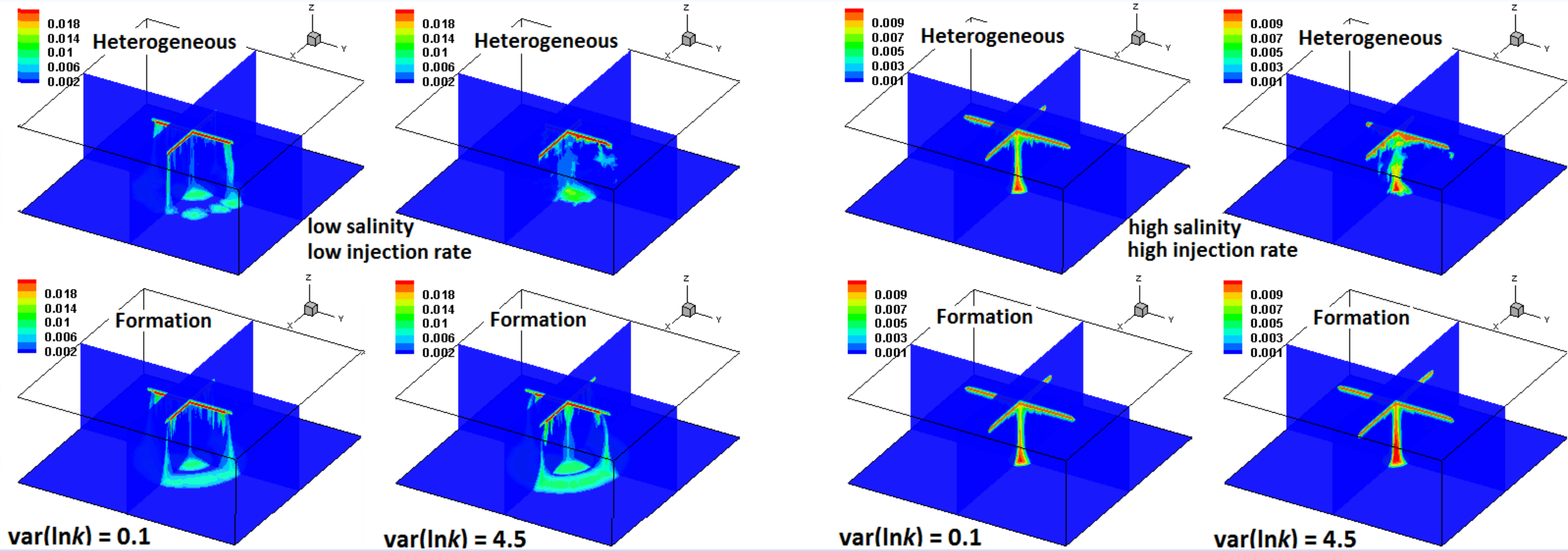

Low salinity (0 Molal) &
Low injection rate (0.252 Mt/yr for 10 yr)

High salinity (4.0 Molal) &
High injection rate (0.063 Mt/yr for 40 yr)

Medium caprock permeability 1E-17.5 m^2 and medium temperature gradient -0.0375^{o}c/m

FHM v. 1-Unit Model (scCO2 Plume)

(An identical set of DoE dynamic parameters)

scCO_2 at the end of monitoring

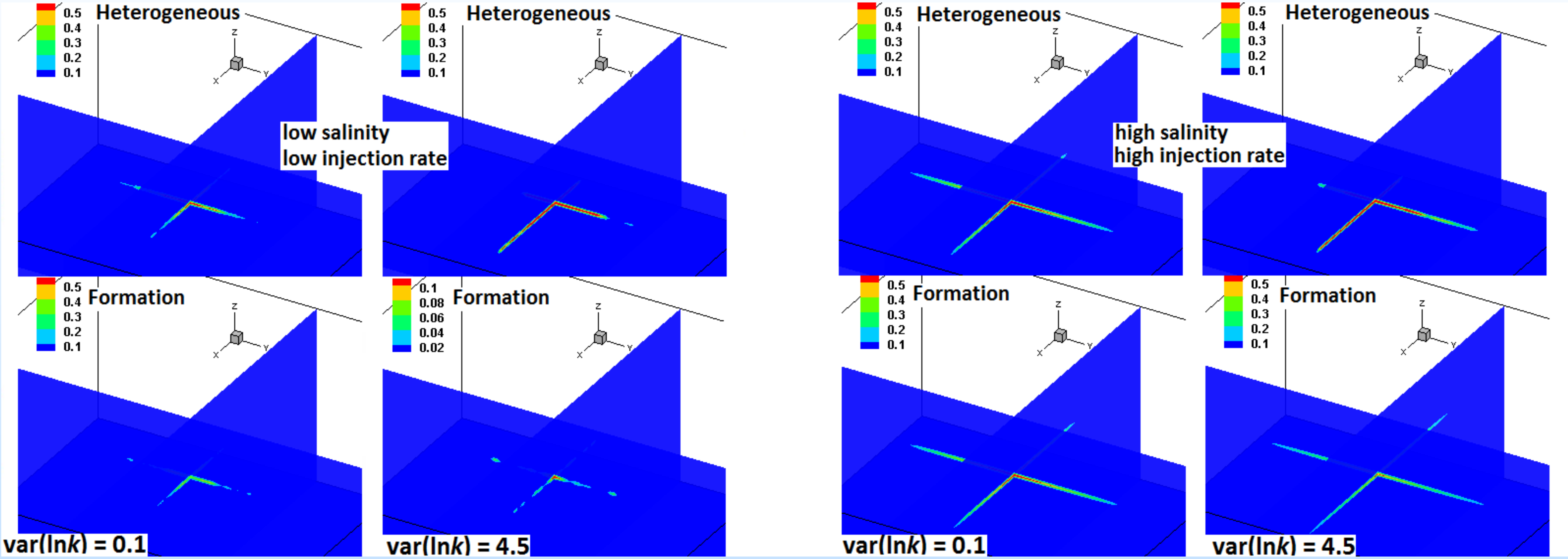

Low salinity (0 Molal) &
Low injection rate (0.252 Mt/yr for 10 yr)

High salinity (4.0 Molal) &
High injection rate (0.063 Mt/yr for 40 yr)

Medium caprock permeability 1E-17.5 m^2 and medium temperature gradient -0.0375^{o}c/m

Design of Experiment (1-Unit; $\sigma^2_{\ln k}$=0.1)

Environmental/engineering factors | Dissolved CO_2 at 2 time scales

Pattern	T_Gradient	Brin_Salinity	K_Cap	Inj_rate	DC_EOI	DC_EOM
−−00	-1	-1	0	0	6.00E+06	4.73E+07
−+00	-1	1	0	0	3.41E+06	1.13E+07
+−00	[illegible]	[illegible]	0	0	5.98E+06	4.75E+07
++00	[illegible]	[illegible]	0	0	2.56E+06	1.89E+07
00−	[illegible]	[illegible]	-1	-1	5.64E+06	2.04E+07
00−	[illegible]	[illegible]	-1	1	5.13E+06	2.14E+07
00+	[illegible]	[illegible]	1	-1	3.94E+06	1.72E+07
00+	[illegible]	[illegible]	1	1	4.09E+06	1.83E+07
−00	[illegible]	[illegible]	0	-1	4.80E+06	1.89E+07
−00	[illegible]	[illegible]	0	1	4.34E+06	2.00E+07
+00	[illegible]	[illegible]	0	-1	4.79E+06	1.88E+07
+00	[illegible]	[illegible]	0	1	4.31E+06	1.98E+07
0−−0	[illegible]	[illegible]	-1	0	7.28E+06	4.85E+07
0−+0	[illegible]	[illegible]	1	0	5.50E+06	4.66E+07
0+−0	[illegible]	[illegible]	-1	0	4.00E+06	1.27E+07
0++0	[illegible]	[illegible]	1	0	2.92E+06	9.92E+06
−0−0	[illegible]	[illegible]	-1	0	5.28E+06	2.10E+07
−0+0	[illegible]	[illegible]	1	0	3.91E+06	1.77E+07
+0−0	[illegible]	[illegible]	-1	0	5.27E+06	2.08E+07
+0+0	[illegible]	[illegible]	1	0	3.89E+06	1.75E+07
0−0−	0	-1	0	-1	6.63E+06	4.86E+07
0−0+	0	-1	0	1	5.92E+06	4.71E+07
0+0−	0	1	0	-1	3.62E+06	1.10E+07
0+0+	0	1	0	1	3.33E+06	1.18E+07
0000	0	0	0	0	4.43E+06	1.92E+07

- *The DoE runs for a given static model use the same injector, injecting the same amount of CO_2, and assuming the same BC.*
- *Identical DoE is used for all static models.*
- *Total simulations = 25 (DoE) x 4 (models) x 3 (lnk variances) =300*

Parameter Ranking (1-Unit; $\sigma^2_{lnk}=0.1$)

Outcome: dissolved CO_2

End of Injection

Response DC_EOI

Sorted Parameter Estimates

Term	Estimate	Std Error	t Ratio	Prob>|t|
Brin_Salinity	-1455849	46624.88	-31.22	<.0001*
K_Cap	-695494.1	46624.88	-14.92	<.0001*
Inj_rate	-192151.7	46624.88	-4.12	0.0014*
Brin_Salinity*Brin_Salinity	236487.8	69937.33	3.38	0.0055*
K_Cap*K_Cap	198258.53	69937.33	2.83	0.0150*
T_Gradient*Brin_Salinity	-207500	80756.67	-2.57	0.0246*
Inj_rate*Inj_rate	160816.72	69937.33	2.30	0.0402*
Brin_Salinity*K_Cap	174539.93	80756.67	2.16	0.0516
K_Cap*Inj_rate	167153.43	80756.67	2.07	0.0607
T_Gradient	-78550.98	46624.88	-1.68	0.1178
Brin_Salinity*Inj_rate	105025.44	80756.67	1.30	0.2178
T_Gradient*T_Gradient	-88514.77	69937.33	-1.27	0.2297
T_Gradient*Inj_rate	-7732.4	80756.67	-0.10	0.9253
T_Gradient*K_Cap	-982.4175	80756.67	-0.01	0.9905

End of Monitoring

Response DC_EOM

Sorted Parameter Estimates

Term	Estimate	Std Error	t Ratio	Prob>|t|
Brin_Salinity	-17504594	439487.3	-39.83	<.0001*
Brin_Salinity*Brin_Salinity	10830867	659230.9	16.43	<.0001*
K_Cap	-1464021	439487.3	-3.33	0.0060*
T_Gradient*Brin_Salinity	1850000	761214.3	2.43	0.0317*
T_Gradient	594637.13	439487.3	1.35	0.2010
T_Gradient*T_Gradient	597259.77	659230.9	0.91	0.3828
Brin_Salinity*Inj_rate	568314.6	761214.3	0.75	0.4697
Inj_rate	288895.85	439487.3	0.66	0.5234
K_Cap*K_Cap	-332572	659230.9	-0.50	0.6231
Brin_Salinity*K_Cap	-220789.7	761214.3	-0.29	0.7767
Inj_rate*Inj_rate	-173873.9	659230.9	-0.26	0.7964
T_Gradient*Inj_rate	-22957.33	761214.3	-0.03	0.9764
K_Cap*Inj_rate	18943.775	761214.3	0.02	0.9806
T_Gradient*K_Cap	15214.875	761214.3	0.02	0.9844

CO_2 Simulation: Mineral Trapping

- Reactive minerals in sandstone such as chlorite and plagioclase can provide cations such as Mg^{2+}, Fe^{2+}, and Ca^{2+}, which are essential chemical components for forming carbonate precipitates during GCS (Xu et al., 2012).

- The reactions between cations and CO_2 forms carbonate minerals (e.g., calcite, siderite, magnesite, and ankerite) to trap CO_2 as precipitates.

- When modeling mineral storage, uncertainty exists in (1) reactive mineral volume fractions; (2) reactive surface areas; (3) kinetic rate parameters; (4) thermodynamic database.

- When we have multiple static models, uncertainty also exists in upscaling geochemical reaction parameters (e.g., mineral volume fractions, reactive surface areas).

Bulk Mineralogy (Same for all Static Models)

Mineral	Formula	Init VF (%)
Quartz	SiO_2	43.04
Calcite	$CaCO_3$	4.22
K-Feldspar	$KAlSi_3O_8$	15.78
Plagioclase	$(Na_{0.75},Ca_{0.25})(Al_{1.25},Si_{2.75})O_8$	4.07
Illite	$K_{0.6}(Mg_{0.25}, Al_{1.8})(Al_{0.5}, Si_{3.5})O_{10}(OH)_2$	4.01
Hematite	Fe_2O_3	1.60
Chlorite	$(Mg_{2.5}, Fe_{2.5}, Al)(Al, Si_3)O_{10}(OH)_8$	7.19
Albite	$NaAlSi_3O_8$	0
Dawsonite	$NaAlCO_3(OH)_2$	0
Kaolinite	$Al_2Si_2O_5(OH)_4$	0
Siderite	$FeCO_3$	0
Ankerite	$Ca(Mg_{1.3}, Fe_{0.7})(CO_3)_2$	0
Magnesite	$MgCO_3$	0
Na-Smectite	$Na_{0.290}(Mg_{0.26}, Al_{1.74})(Al_{0.03}, Si_{3.97})O_{10}(OH)_2$	0
Ca-Smectite	$Ca_{0.145}(Mg_{0.26}, Al_{1.74})(Al_{0.03}, Si_{3.97})O_{10}(OH)_2$	0
Dolomite	$(CaMg)(CO_3)_2$	0

Mineral Mass Balance (1-unit model)

CO_2 is injected at 10 kg/s for 10 years or 3.1536*10^9 kg

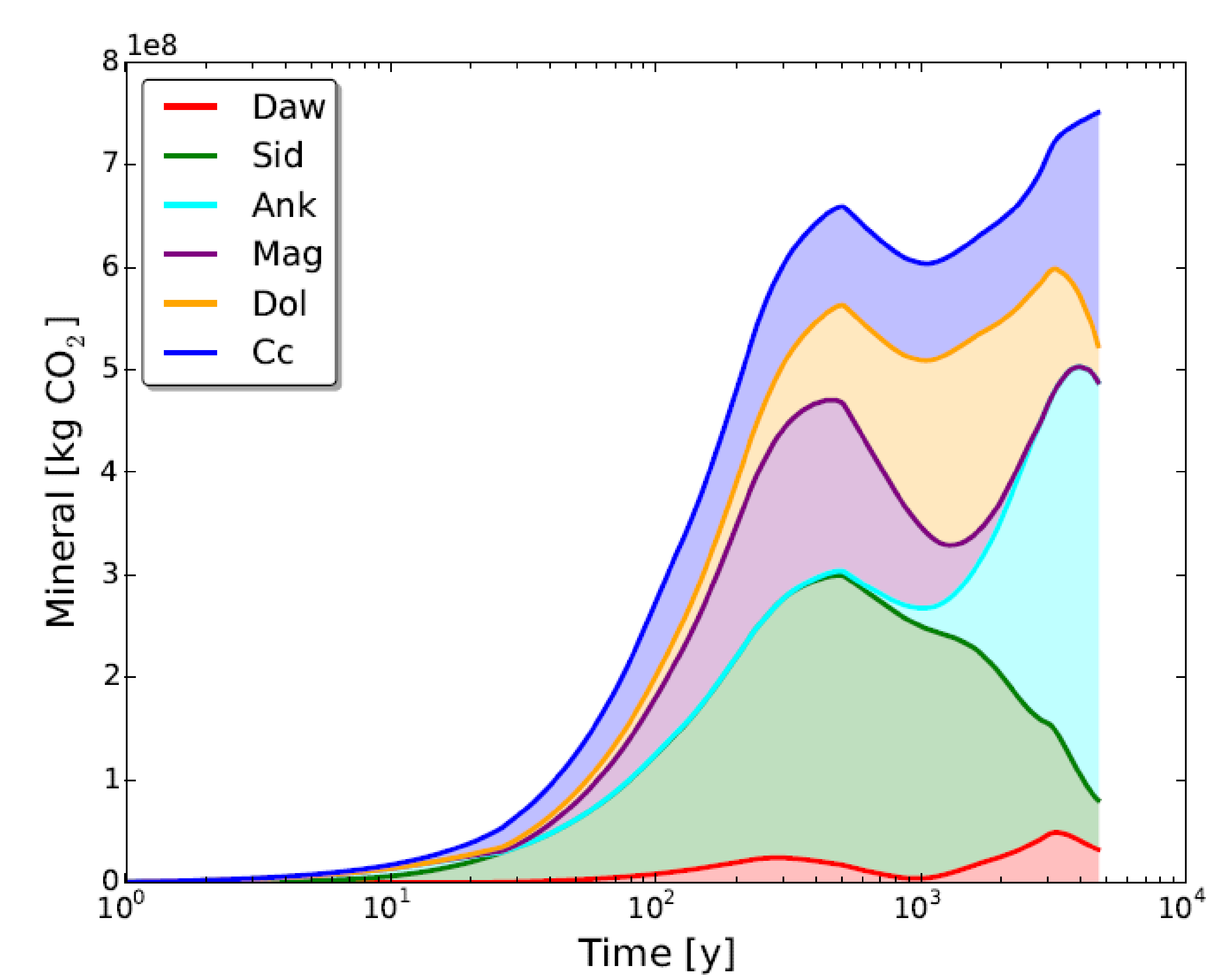

After 40,000 years, around 10% of the injected CO_2 has been transformed to carbonate minerals

Deep Storage: Onshore

Onshore simulations using the Span-Wagner EOS suggest that a very low geothermal gradient is needed to develop conditions suitable for gravity-stable injection. Such cool conditions may exist in parts of the continental US. We're collecting data from these locations to obtain precise in-situ reservoir T and P data before repeating the simulations.

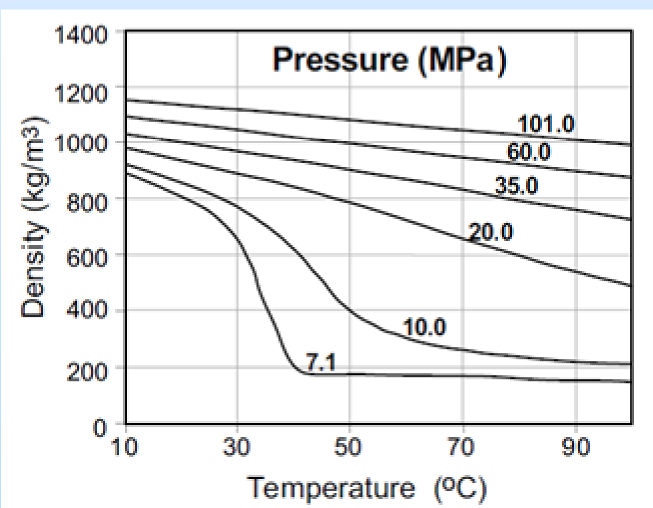

Bachu & Stewart (2002)

MIT (2006)

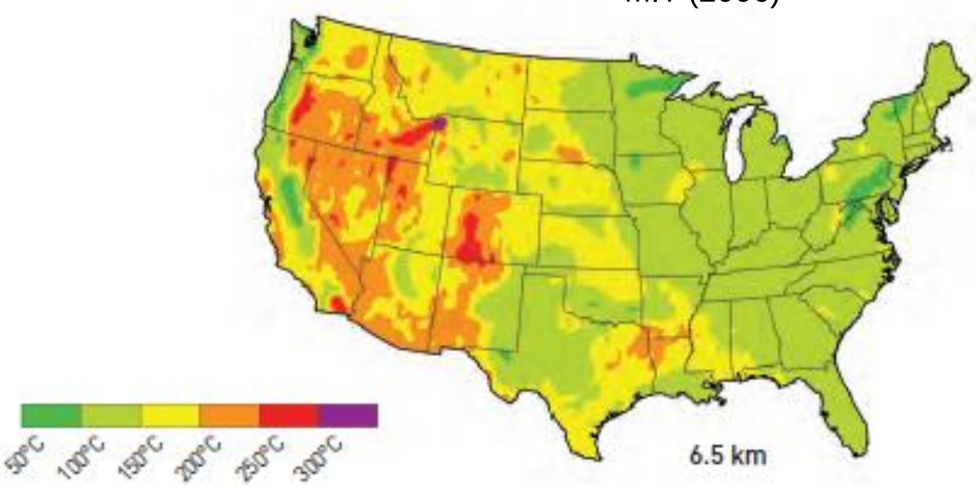

Figure 1.4 Temperatures at a depth of 6.5 km.

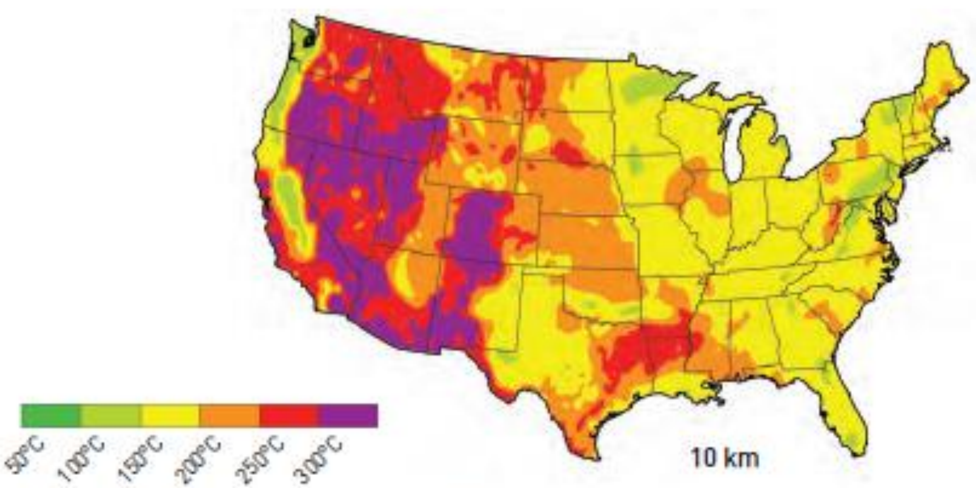

Figure 1.5 Temperatures at a depth of 10 km.

Deep Storage: Off-shore

Personal communicatior Phil Stauffer, F (2015); Also, L et al. (2013)